LARGE-SCALE TESTING OF A STEEL-CONCRETE COMPOSITE FLOOR SYSTEM UNDER COLUMN LOSS SCENARIOS

BY

ERIC STOLOW JOHNSON

THESIS

Submitted in partial fulfillment of the requirements
for the degree of Master of Science in Civil Engineering
in the Graduate College of the
University of Illinois at Urbana-Champaign, 2014

Urbana, Illinois

Adviser:

Professor Larry Fahnestock

ABSTRACT

Large-scale floor system tests concluded a collaborative research project that studied the structural integrity of steel gravity framing systems composed of steel beams and girders with composite concrete slab on steel deck. Steel simple beam-column connection tests were conducted at the University of Washington, steel-concrete composite slab tests were conducted at Purdue University, and complete floor system tests were conducted at the University of Illinois at Urbana-Champaign. The complete floor system tests evaluate gravity systems subjected to severe demands consistent with column loss scenarios, complementing the previously completed component tests. The floor system tests were conducted at half scale on a three-bay square configuration that considers interior, exterior and corner column loss scenarios. The 3-bay by 3-bay configuration was chosen so that multiple tests could be conducted using one structure. For each test, the bays adjacent to the removed column were incrementally loaded with distributed load until the floor could not support more load. These experiments provide valuable data that can be used to validate existing numerical models, identify critical limit states, and determine system capacities under various column loss scenarios.

ACKNOWLEDGEMENTS

First and foremost, I would like to acknowledge my advisor, Larry Fahnestock. He has supported and guided me from my first day of graduate school to my final revision of this thesis. He is a truly wonderful advisor. Thank you.

This project was funded and supported by the National Science Foundation (Grant Nos. CMMI-1000926, 0969837, 1000077) and the American Institute of Steel Construction. I would like to acknowledge our colleagues who led other portions of this project: Judy Liu and Timothy Francsisco at Purdue University and Jeffrey Berman and Jonathan Weigand at the University of Washington. I also would like to acknowledge Joseph Main of NIST for his ongoing computer modeling of the test specimen.

Many people and groups assisted with the project from design through construction and testing. Through the whole process, we were assisted by Timothy Prunkard and the staff of the Newmark Civil Engineering Lab. Also throughout the process, I had many undergraduate assistants helping with instrumentation, construction, testing, and other miscellaneous jobs required for the project: Hong Kim, Hareem Dar, Monica Hue, Enji "Paul" Papazisi, Yingchao Sun, Nimit Bhatia, Jeremy Kaiser, Anna Molins Estellés, Anthony Ali, and Xuguang Feng.

We were also assisted by some of my graduate student colleagues. Alvaro Quinonez took lead in the summer of 2012 while the project transitioned from Jeffrey Meissner to myself. Daniel Borello, Timothy Gregor, and Derek Kozak assisted with the column removal tests.

I would like to thank Donald Marrow of the Newmark Lab staff and Michael Bletzinger in the Illinois NEES office for their assistance with instrumentation and data collection. They are the ones who wrote the data collection program in Labview.

Many contractors and university departments provided construction and other support services. From the University, Jill Maxey, Associate Director for Space Analysis, and Greg Larson, Director of Facilities of the College of Engineering, helped secure the university-owned lot used for the tests. Several different groups from the University of Illinois Facilities and Services Department helped in many stages of the project: Operators Shop 37, Transportation Shop G3, Iron Workers Shop 50, Cement Finishers Shop 49, Electricians Shop 3, and Laborers Shop 7. From outside of the university: Tefft Bridge & Iron fabricated the steel frame components, Canam donated the corrugated metal decking, Petry-Kuhne Co. provided stud

welding services, Prairie Material supplied the concrete, Custom Service Crane Inc. provided the cranes for the tests, and the Illinois American Water Company provided access to a fire hydrant and supplied the water used for loading the test specimen.

TABLE OF CONTENTS

CHAPTER 1 - INTRODUCTION[1]

1.1 MOTIVATION

Beyond design of modern buildings for structural efficiency, design for redundancy and resilience in case of events like blast and impact is needed. The bombing and subsequent disproportionate collapse of the Murrah Building (completed in 1977) in Oklahoma City on April 19th, 1995, the collapse of the World Trade Center towers (completed in 1973) on September 11th, 2001, and the bombings of several U.S. government and military installations worldwide have created a great interest in blast loading and disproportionate collapse research. Government and military buildings are now constructed to meet the requirements of relatively new standards such as DoD (2013) and GSA (2003) that are intended to improve their structural resilience in the event of localized damage.

Although these new standards may be applied to a non-government building if the owner desires, design for enhanced integrity is atypical in standard commercial and residential buildings. For modern steel structural systems, a common configuration is either moment frames on the perimeter or braced frames around the core to resist lateral loads, with the balance of the building being gravity framing. Gravity framing commonly comprises steel beams and girders, simple shear connections and a composite concrete slab on steel deck. The structural integrity of these steel-concrete composite floor systems is not well understood when they are subjected to severe localized damage such as column loss. In particular, large-scale experimental data is needed for these systems. Experiments on steel-concrete composite floor systems have only begun to be conducted recently, since lack of structural redundancy is a relatively new problem derived from the increasing economy and efficiency of building design and construction.

1.2 CURRENT BUILDING CODES FOR PROGRESSIVE COLLAPSE

In the U.S., the most current design document for preventing progressive collapse is the 2013 update of the Department of Defense *United Facilities Criteria (UFC) 4-023-03 Design of Buildings to Resist Progressive Collapse*. This code applies to government and military facilities,

[1] Portions of this chapter have been adapted from Johnson et al. (2014)

not to the typical office and residential buildings that are the focus of this research at the University of Illinois. It is helpful, however, to understand the overarching strategies and specific requirements for designing resilient structures so that they may be applied to private sector construction if desired.

UFC 4-023-03 includes three different methods to provide progressive collapse protection:

> • Tie Forces, which prescribe a tensile force strength of the floor or roof system, to allow the transfer of load from the damaged portion of the structure to the undamaged portion,
> • Alternate Path method, in which the building must bridge across a removed element, and.
> • Enhanced Local Resistance, in which the shear and flexural strength of the perimeter columns and walls are increased to provide additional protection by reducing the probability and extent of initial damage. (UFC 4-023-03 1-4)

The tie force method is considered indirect, where strength is added to the design but no specific damage is considered in the design process. The alternate path method and enhanced local resistance are direct methods, where specific damage is anticipated during the design process.

1.2.1 TIE FORCES

The tie force method requires three horizontal ties, longitudinal, transverse, and peripheral, as well as vertical ties for columns and bearing walls.

> Unless the structural members (beams, girders, spandrels) and their connections can be shown capable of carrying the required longitudinal, transverse, or peripheral tie force magnitudes while undergoing rotations of 0.20-rad (11.3-deg), the longitudinal, transverse, and peripheral tie forces are to be carried by the floor and roof system. Acceptable floor and roof systems include cast-in-place concrete, composite decks… (UFC 4-023-03 3-1)

For design, the factored uniform floor load is $w_f = 1.2D + 0.5L$ and for non-uniform loading within 25% of the minimum load, an effective uniform load is used that is the total non-uniform load divided by the floor area. Another relevant part of the tie force method is that steel-member-

to-concrete-slab connections (shear studs) in composite floors must be sufficiently strong to prevent the steel member from falling to the space below when the floor slab is acting as the tie.

1.2.2 ALTERNATIVE PATH METHOD

The alternative path method requires the structural elements to be strong enough to bridge across damaged or removed elements, particularly columns and bearing walls. The structural elements are divided into primary and secondary components. Primary elements connect directly to vertical elements while secondary elements connect to primary elements but do not directly provide resistance to collapse of the vertical elements. Material properties, component force, and deformation capacities must be evaluated to determine the design of the primary bridging elements. The quantity and location of removed vertical elements considered in design depends on the occupancy category of the building; more vital buildings have stricter requirements for collapse resistance.

1.2.3 ENHANCED LOCAL RESISTANCE

Enhanced local resistance (ELR) is used in certain occupancy categories where a ductile, flexural, failure mechanism must form if a column or wall is loaded laterally, as from a bomb blast or crash. The locations of ELR design are determined by occupancy category. The locations range from just the corner and penultimate perimeter columns and bearing walls of the first story to every perimeter column or every perimeter and penultimate bearing wall in the case of one-way slabs.

1.3 CASE STUDIES AND PAST RESEARCH

The following survey of case studies and research shows how older buildings are more resilient to localized damage while newer and more efficient buildings may not be. On July 28, 1945 a B-25 bomber crashed into the 79th floor of the Empire State Building (completed in 1931). The event was well summarized by Levy and Salvadori (1992). Beyond the immediate damage to the impact area and the elevator shaft, there was no additional damage to the building structure and no disproportionate collapse. This incident demonstrates the resilience of older steel buildings. Like many older buildings, the Empire State Building has moment-resisting, riveted connections. Designed and built before computers and today's advanced metallurgical practices, the building was designed conservatively, with much greater load capacity than required, allowing loads to redistribute into the undamaged columns, beams, and girders.

Recent column removal tests by Song et al. (2010) further show how older building structures are resilient to progressive collapse. Columns were removed from two steel frame buildings with masonry infill partitions that were built in 1951 and 1968. The older building saw very little deformation when four columns had been removed while the newer building failed GSA progressive collapse requirements for deflection and rotation, but did not actually collapse.

Over the past several years, tests of small modern steel floor systems have begun adding to the body of knowledge of system integrity. Astaneh-Asl, et al. (2001) tested an edge column of a full-scale composite floor specimen by pulling down the column. The maximum load in the column was 63 kips, equivalent to a distributed load of 300 psf on the floor. The results of this one test suggested that the floor system could resist progressive collapse. More recently, Jahromi, et al. (2012) loaded a small, full-scale composite floor specimen with distributed load to evaluate interior column loss, finding that the floor could resist loads up to 1.6 times the progressive collapse design load. Subsequent interior and edge column removal tests, as presented at the 2014 Structures Congress, resulted in floor capacities greater than 150 psf. While it is clear that older buildings may in certain situations have the resiliency to prevent collapse after moderate structural damage, more experimental evidence is needed to evaluate the resilience of buildings with modern structural systems.

1.4 NEW RESEARCH

Research at the University of Illinois aimed to provide additional experimental data to more comprehensively understand system behavior while eliminating some of the shortcomings of the previous research. Astaneh-Asl et al. did not use distributed loads on their floor specimen and Jahromi et al. used a full-scale design with short spans that may not reflect the performance of more common floor spans. The experimental tests at Illinois were conducted on a half-scale specimen in an effort to capture realistic force transfer mechanisms and system kinematics. Distributed load was applied on the floor instead of pulling on the removed column to more accurately represent actual floor loading. The Illinois test specimen was also much larger, at three-by-three bays, allowing system effects to contribute to the behavior of the loaded floor bays with column removal. The experimental results will be used to validate existing modeling approaches, including those developed at the National Institute of Standards and Technology (NIST) by Main and Sadek (2012) so that other connection and system configurations can be

analyzed, and recommendations can be made to enhance the integrity of steel-concrete composite floor systems.

The tests described in this thesis are the culmination of a multi-year, collaborative effort to understand, at multiple levels of detail, the behavior of a steel-concrete composite floor system that experiences column loss (Weigand et al., 2013). Connection sub-assemblage experiments at the University of Washington addressed the behavior and robustness of single-plate and bolted-angle shear connections under combined axial tension and large rotation. Uniaxial tests of slab and steel decking components at Purdue University helped characterize localized slab behavior. Work to develop and validate modeling approaches based on connection and slab component test results is ongoing.

CHAPTER 2 - EXPERIMENTAL METHODS

2.1 SPECIMEN CONFIGURATION

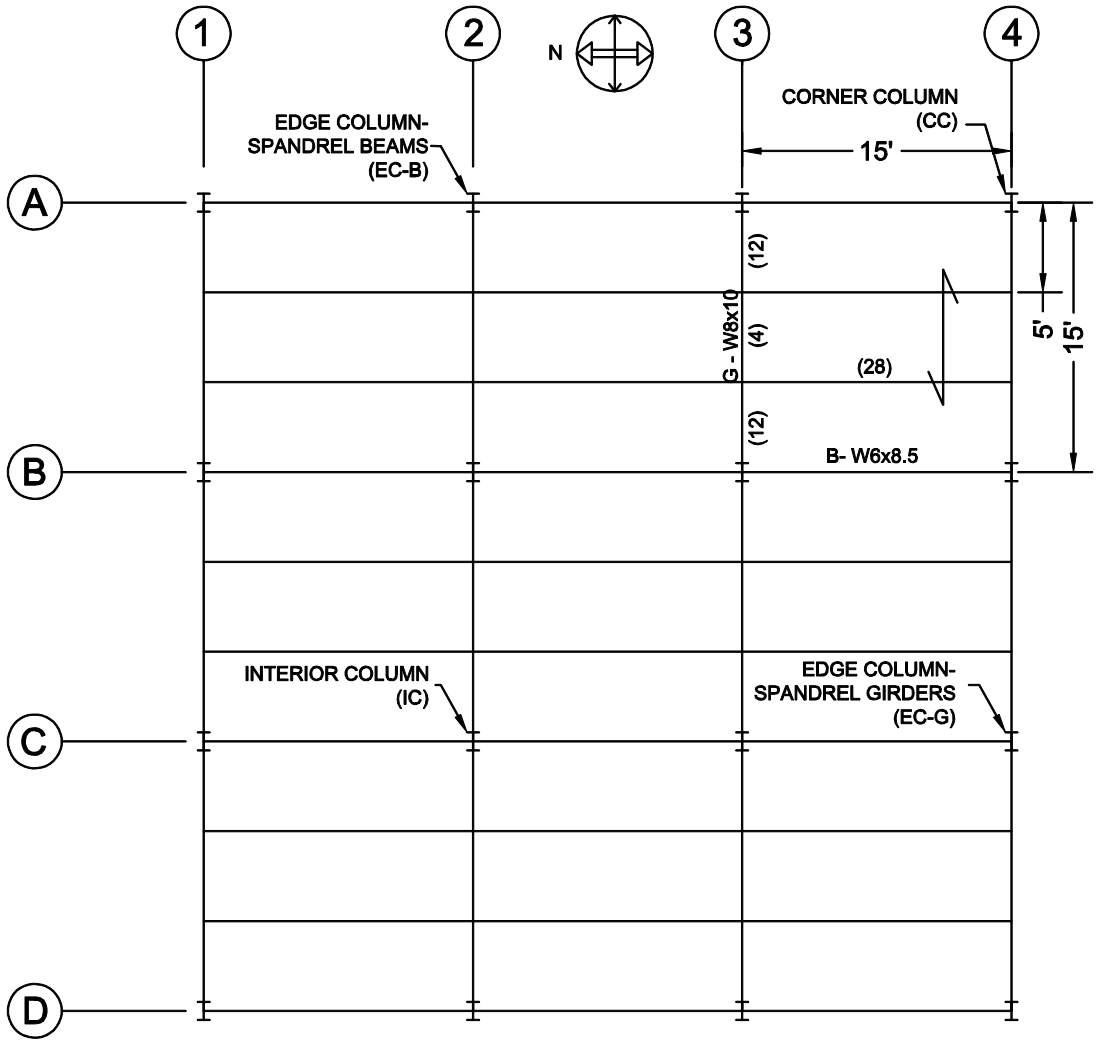

Figure 2.1 Floor System Layout

2.1.1 DESIGN LOADS

The test specimen was a half-scale, 3-bay by 3-bay, partially-composite steel gravity frame with a concrete slab on corrugated steel deck. (Figure 2.1) This half-scale system was derived from a full-scale system, and connection and member limit states were correlated between the full and half-scale designs (Meissner, 2012). The full-scale specimen was designed to resist typical office building gravity loading: 92 psf total dead load and 50 psf live load. The Load and Resistance Factor Design (LRFD) strength combination (1.2D+1.6L) is 190 psf. LRFD load combinations that include transient loads such as wind and earthquakes take the form

1.2D+0.5L+1.0*(transient event load). In these tests, column removal was considered the transient (or extreme) event, and therefore the benchmark gravity load to compare to the floor load at failure was 1.2D+0.5L = 135 psf. While the geometries of the specimen scaled down, the load pressure remained unchanged because the total load was reduced with the reduced area of the floor.

2.1.2 SPECIMEN SCALING

The full-scale design (Figure 2.2) was 90 ft. square with 30 ft. bays. W18x40 girders connected to W14x90 columns. There were two W16x26 in-fill beams per bay and W16x26 beams also connected to the columns. The floor was a 3-1/4 in. lightweight concrete slab on 3 in. corrugated galvanized steel decking. To achieve partial composite action, the beams had 28 shear studs, one for every deck rib. The girders had 18 studs on their outer thirds and 4 studs in the middle third.

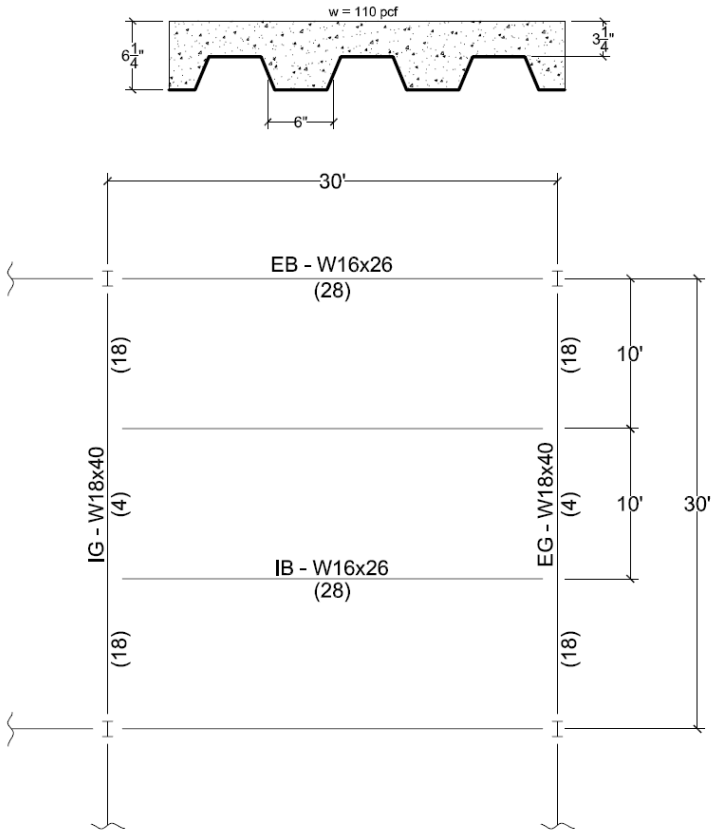

Figure 2.2 Full-scale Specimen Bay Design

The design was scaled so that the test specimen would fit the testing site constraints and not exceed the project's budget. The general dimensions of the specimen were scaled by half

(Figure 2.3) so that the floor became 45 ft. square with 15 ft. bays and the floor had 1-5/8 in. concrete slab on 1-1/2 in. corrugated, galvanized steel decking. The concrete was reinforced with 6 x 6 W1.4/W1.4 (10 gauge) welded wire fabric. As mentioned before, the distributed floor loads remained unchanged. The half-scale member dimensions were chosen such that the following three conditions were nominally satisfied: 1) the ratios of demand to capacity for moment and shear were equal between full and half scale, 2) the level of partial composite action in the floor remained constant, 3) the ratio of allowed to predicted deflections was held constant. The final half-scale design had W6x8.5 beams (fabricator provided W6x9), W8x10 girders, and W8x24 columns. The shear studs were 3/8 in. diameter and 2-5/8 in. long. The beams had 29 studs, one per rib, and the girders had 14 studs in the end thirds and 2 in the middle third.

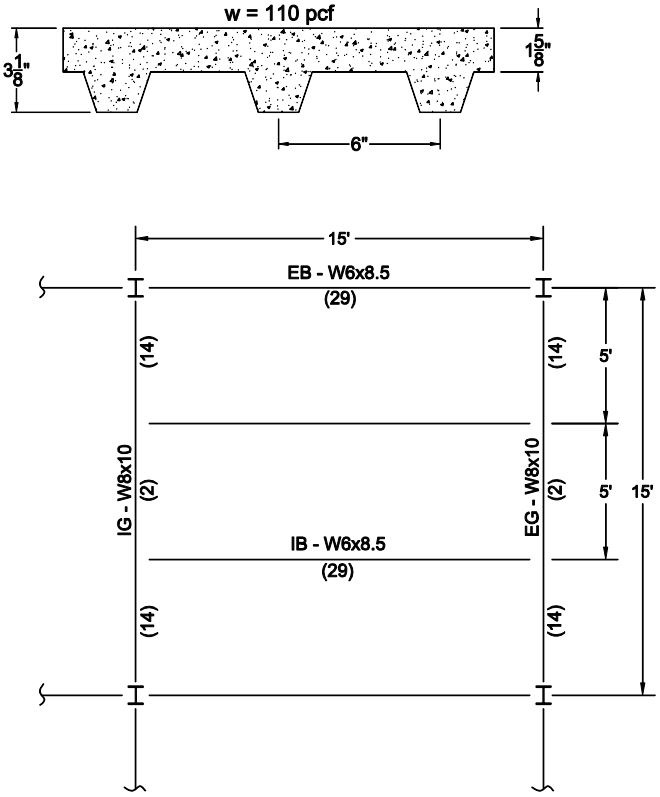

Figure 2.3 Half-Scale Specimen Bay Design

Three connection types were used for the beam-to-column, beam-to-girder, and girder-to-column connections. The connection types were chosen in consultation with a project advisory committee sponsored by AISC. Given the demands delivered to the connections from the members, the connections were designed considering all limit states defined by AISC 360-10 (2010). The connections were scaled so that the ratio of the capacity of each limit state to the

capacity of the governing limit state was roughly constant between the full- and half-scale configurations. All bolted half-scale connections used ⅜ in. diameter A449 bolts with the threads included in the shear plane (N condition). Although the mechanical properties of A449 steel are essentially the same as A325 steel, the A449 bolts used in this testing program were threaded along the full length of the shank. The beam-to-column connection (Figure 2.4) was an unstiffened extended single shear plate welded to the column web with three bolts connecting to the beam web. The girder-to-column connection (Figure 2.5) was a double-angle with three bolts through the girder web and three bolts through each angle into the column flange which were offset from the girder bolts. The beam-to-girder connection (Figure 2.6) was a single-angle with three bolts in the beam web aligned with three bolts through the girder web. The filler beams were coped on the top where they met the girders.

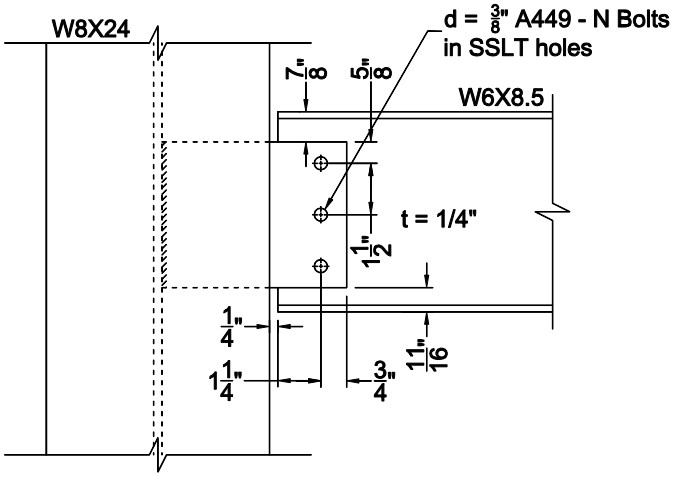

Figure 2.4 Half-scale Beam-to-Column Shear Tab Connection

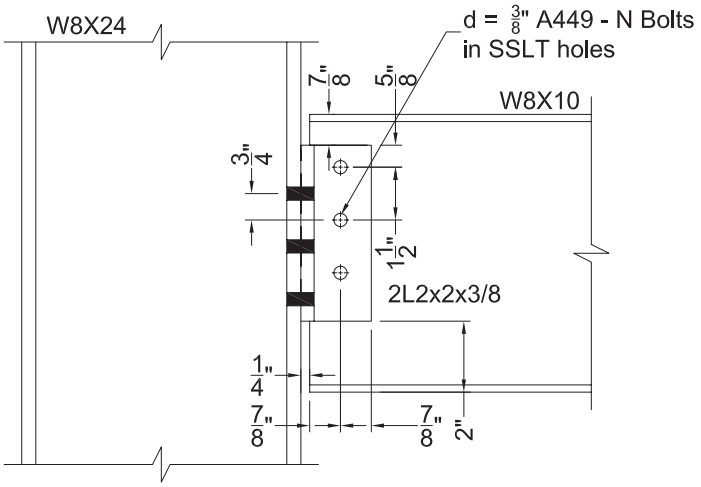

Figure 2.5 Half-scale Girder-to-Column Double-Angle Connection

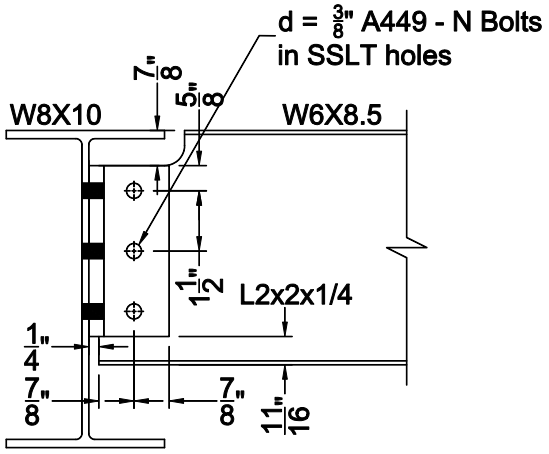

Figure 2.6 Half-scale Beam-to-Girder Single-Angle Connection

2.1.3 FOOTINGS

The 16 columns were supported by normal-weight concrete footings placed on grade. The footings were 5 ft. square and nominally 2 ft. thick, though thickness varied to ensure the structure was level over the sloping land surface. The footings were oversized to avoid sliding during the column removal tests and to eliminate the risk of settlement since there was no geotechnical survey of the site. The concrete strength required to resist the column loads was less than 4000 psi, but the concrete was specified to be 5000 psi to ensure that the anchor rods in safety restraint columns adjacent to the exterior column removal locations would not pull out of the concrete. Eight cylinders tested after 28 days showed an average strength of 4812 psi. The test results were variable and below 5000 psi most likely because the cylinders were not carefully filled. These results were not concerning since 4812 psi was acceptable for all limit states.

2.1.4 LATERAL BRACING

Diagonal braces were added to the steel frame to provide stability and further resist local lateral loads from the catenary action in beams and girders during the column removal tests. These braces created equilibrium within the specimen, keeping the footings from sliding. The braces were double angle members, 2L-3½x3½x3/8 with two intermediate connectors. The braces were connected to gusset plates welded to the columns by three 1 in. slip-critical bolts at each end of a brace.

2.1.5 COLUMN REMOVAL DETAILS

Four columns had sections that could be removed to perform the testing. The corner column removal location was grid point A4, the edge column with spandrel beams was at A2, the edge column with spandrel girders was at C4, and the interior column was at C2 (pictured in Figure 2.7). The removable sections of the columns were 3 ft. long, centered between the footings and the floor beams. The removable section was attached by four bolts through plates welded to the ends of the W-sections of the column. Teflon pads separated the steel plates of each column section so the column section could be easily removed during testing.

Figure 2.7 Removable Interior Column

2.1.6 SAFETY FEATURES

Because the specimen was to be tested to failure, a number of safety mechanisms were installed on the specimen. One of the expected failure modes was the failure of the bolted beam-to-column and girder-to-column connections. Seats made of channel sections were welded beneath the beams and girders to prevent the beams and girders from falling to the ground in the

event of connection failure. With the seats, seen in Figure 2.7, the beams and girders could only fall a few inches.

Cable slings were installed to connect the edge girders to the filler beams in case of failure at the single-angle beam-to-girder connections (Figure 2.8a). The slings were attached to the structural members with bolts through the member flanges. It was later noted that the loss of section area could reduce the flexural strength of the members. Calculations showed that the only locations where premature yielding was a possibility were on the interior girders. The slings were removed from the interior girders and 12 in. flange plates were welded onto the bottom flange of the girders at the hole locations to bring the flexural strength back to the design strength.

Restraint columns were used for the corner and edge column removal tests (Figure 2.8b). These columns were attached to the footings outside of the specimen columns and used to prevent the upper column section from kicking out beyond the bounds of the specimen during testing.

A wooden railing was installed around the perimeter of the floor, which was approximately 8 ft. above the ground, to provide safety for people working on the floor.

Figure 2.8 (a) Girder-to-Beam Safety Cable Sling (b) Restraint Columns

2.2 INSTRUMENTATION

The test specimen was monitored by a variety of instruments capable of capturing a range of behavior from global system deformation to local strains and connection deformation. Some instruments were used in the same location for every test, some moved to a new location between tests, and others were only used once.

Linear strain gauges measured strain in the top and bottom flanges of a subset of the beams and girders under the loaded floor. Strain was measured in different locations for each test.

Strain was also measured in the deck. Strain rosettes were attached to the steel deck and embedment strain gauges were tied to the welded-wire mesh and embedded in the concrete slab (Figure 2.9). The rosettes and embedment gauges were placed in a line from the removed column to the column diagonally across the bay. They were oriented so that strain was measured in line with the floor grid (0º and 90º) and along the diagonal (45º).

Figure 2.9 Embedment Strain Gauges Arranged as a Rosette

Inclinometers were attached to the columns, beams, and girders to measure rotation of the members and connections as the floor deformed. The inclinometers were moved after each test in order to measure rotation at the critical points in the next test. The inclinometers were mounted with screws onto small plywood plates that were bolted into coupler nuts that were welded to the steel members (Figure 2.10).

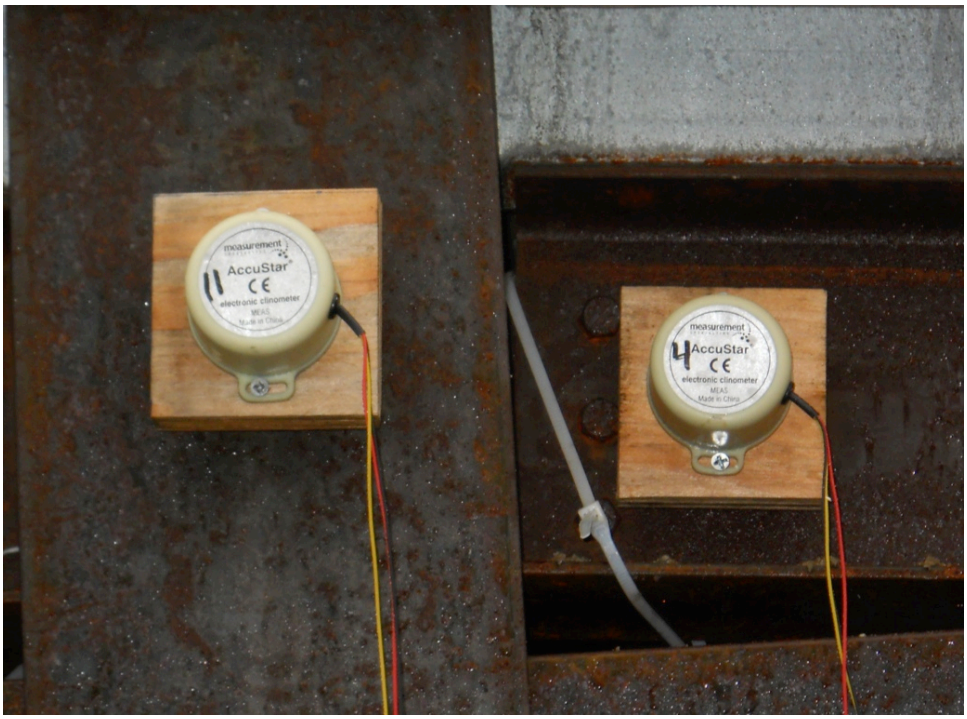

Figure 2.10 Inclinometers Mounted on Test Specimen

String potentiometers (string pots) were used in many different locations to measure displacement. Initially, string pots were used to measure the global displacement of the whole floor system in plan. After the first test, it was clear that these global measurements were not a valuable use of instrumentation. The global deformations ranged from negligible to fractions of an inch. In the subsequent tests, those string pots were used to measure local displacements at the connections between the flexural members and the columns (Figure 2.11). Additional string pots measured vertical displacement. Two were used (for redundancy) to measure the vertical displacement at the removed column location. In some tests, vertical displacement was also measured at the midspan of the beams and girders that attached to the removed column.

Figure 2.11 String Potentiometer Installed to Measure Local Displacements at a Beam-to-Column Connection

The final type of instrument was a strain gauge full bridge (Wheatstone Bridge) used to measure the axial force in the columns and diagonal braces. These bridges were wired using four linear strain gauges configured so that flexure and temperature effects would cancel, leaving only pure axial tension or compression in the measurement signal. Every column and brace had a full bridge and load data was collected for every bridge for every test. The removed columns had two bridges each: one was between the footing and the floor to measure load when the column was intact and another was above the floor to measure the load being held by the crane. The crane load was also measured by reading the crane's built-in instrumentation and by using a digital load cell placed between the crane hook and the column.

The data acquisition system (DAQ) used hardware from National Instruments and code written in Labview. Several thousand feet of four-conductor, 22 AWG shielded cable attached the instruments to the DAQ in an office trailer at the test site.

2.3 SPECIMEN CONSTRUCTION

Since the goal of this project was to understand the structural integrity of actual building floor systems, the specimen was constructed using actual construction practices and not ideal laboratory conditions. As a result, minor mistakes were tolerated, field adjustments were made to accommodate small fit-up issues, and the specimen was not cleaned during the erection process

(e.g., typical construction debris was not cleaned out of the corrugated steel deck before placing the concrete).

2.3.1 SITE CHARACTERISTICS

The test site was an empty lot owned by the University of Illinois at the corner of Main St. and Goodwin Ave. in Urbana, IL. The lot was located on the far side of the Siebel Center from Newmark Civil Engineering Laboratory and was approximately 190 ft. by 115 ft.

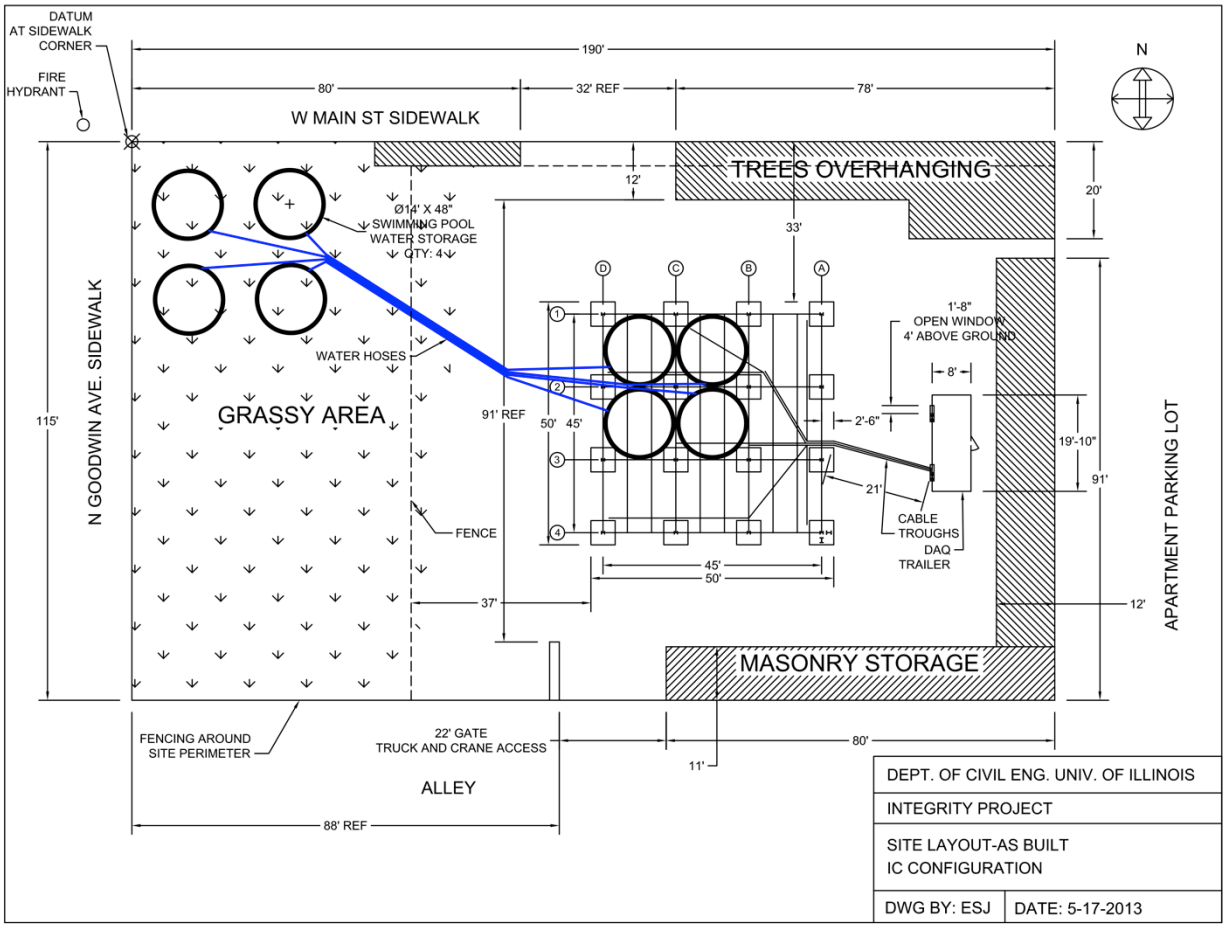

Figure 2.12 Test Site Layout with Loading Pools Arranged for the Interior Column Test

Figure 2.12 displays the general site layout. The east portion of the lot was a former parking lot with hard, dense gravel and patches of asphalt still intact. The structure was built on this area because of the flat, hard ground. The west side of the lot was grassy with softer soil. The northwest corner was used for the swimming pools that stored the water because it was close to the fire hydrant that provided the water. The trailer was placed approximately 20 ft. east of the

test specimen and held the DAQ as well as tools and other project materials. Electricians installed a temporary utility pole next to the trailer to provide power for the project.

2.3.2 FOOTING CONSTRUCTION

Footing construction was one of the longest phases of construction. The forms and reinforcement were constructed during summer 2012 and then put in storage for the winter. Due to the long winter, forms were not laid out until April 2013 and the concrete was placed on May 1, 2013. (Figure 2.13)

(a) **(b)**

Figure 2.13 (a) Footing Form with Reinforcing, Column Anchor Rods and Setting Plate Installed (b) Placing Concrete Footings

2.3.3 STEEL CONSTRUCTION

The structural steel was delivered to the site in early March. Most of it was stored onsite until erection in May, but some beams and girders along with the braces were brought into the Crane Bay in Newmark Lab so that strain gauges could be installed prior to erection.

University ironworkers erected the steel framing over a few days in early May 2013 (Figure 2.14), with a few challenges and errors. Some of the setting plates and anchor rods were placed in the footings incorrectly since many of the plates were similar, but mirrored or rotated with varying symmetries. Drilling new holes in the column base plates to fit with as-built anchor rod layouts solved this problem. (Figure 2.15) Additionally, the non-coped beams that framed to the columns were designed with bolt holes slightly off-center. (Figure 2.4) Three of these were installed upside-down since it was difficult for the erectors to tell which way was correct.

Though this problem could not be fixed, it was deemed non-critical since it lowered the deck level along these three beams by only ½ in.

Figure 2.14 Erected Steel Framing

Figure 2.15 New Holes Drilled in Base Plates to Match As-Built Anchor Rod Placement

2.3.4 FLOOR CONSTRUCTION

After erecting the framing, the ironworkers installed the galvanized corrugated steel decking. The decking came in 3 ft. x 15 ft. sheets and was attached to the beams and girders with

puddle welds every three ribs (18 in.). The decking sheets were attached to each other with side-lap screws every 2 to 3 ft.

A specialty contractor was hired to shoot the shear studs (Figure 2.16a). There were several challenges associated with shooting studs on a half-scale floor. First, the decking ribs were only 1-1/2 in. wide, making it difficult to get the stud gun in proper position. There were places where the decking had to be deformed locally to make the rib wider to accommodate the gun. Also, there were places along the girder lines where two pieces of decking overlapped. Stud guns cannot shoot through two layers of decking, so some decking had to be cut away.

(a) **(b)**

Figure 2.16 (a) Contractors Shooting Shear Studs (b) Qualification of Stud Welds

Determining the proper welding settings to correctly shoot the studs required several trial iterations. Moisture on the decking also made it challenging to get solid welds. The standard qualification for shear studs is to use a hammer to beat ten studs in a row to a 45º angle. Even after the studs passed the qualification (Figure 2.16b), there were still problems with studs not welding properly to the beams and girders. Therefore, all studs were nominally tested (not to 45º) by hitting them once with a hammer to make sure they were welded soundly. The feeling of the impact with the hammer was a good way to tell if the weld was solid, especially for the obviously weak studs that knocked off the deck with one hammer hit. Even more effective was listening to the sound of the hammer hit; a long ring with the beam below the stud reverberating

as well indicated a strong weld because it indicated the stud and beam were well connected. Poorly welded studs would make a thudding sound when hit with a hammer. In the end, every stud was checked and deemed intact. After the shear studs were welded, the ironworkers returned briefly to lay out the welded wire fabric, placed on the decking with no chairs, before the concrete slab was placed.

Figure 2.17 Finishers Placing the Concrete Floor Slab

University concrete finishers placed the floor slab on Jun 21, 2013 (Figure 2.17). Three mixers from Prairie Material delivered a total of 20.5 cubic yds. of lightweight concrete. Overstrength is typical in ready-mix concrete so the mix order was specified to have f'_c=3000 psi so that the actual strength would be closer to the desired f'_c=4000 to 5000 psi. Concrete cylinder tests were performed multiple times and are summarized in Table 2.1. A concrete pumper was used since the floor was 8 ft. above the ground. Superplasticizer was added to the mixer to make the concrete pumpable. Slumps ranged from 5 to 9 in. out of the mixer after addition of superplasticizer, but the finishers reported much lower slumps by the time the concrete made it

through the pumping hose and onto the deck for placement. The slab had a fairly rough finish to minimize the slipping hazard when wet. The finishers sprayed curing compound on the surface of the slab to retain the water content during curing. Only one shrinkage crack formed during curing: it ran along the girder line from A3 to B3. The maximum wet weight deflection was in the filler beams and was approximately 0.25 in. or L/720. The beams and girders were not cambered due to their 15 ft. length. Overall, construction took over two months, with many weather-related delays.

2.4 TESTING PROGRAM

The testing program was made up of four individual column removal tests. In each test, the only bays loaded were those directly adjacent to the removed column. The test specimen was arranged so that no floor bay would be loaded twice. The goal was that any given test would not damage the other bays not being loaded. The four column removal tests were, in order, corner column (CC) at A4, edge column with spandrel beams (EC-B) at A2, edge column with spandrel girders (EC-G) at C4 and interior column (IC) at C2. This order progressed the tests from least load to most load, and least damage to most damage; only one bay was loaded for CC, two bays were loaded for EC-B and EC-G, and four were loaded for IC.

2.4.1 LOADING METHOD

The floor bays were loaded with water pumped into swimming pools sitting on the floor. The Intex brand pools with metal frames and plastic liners were circular with 14 ft. diameter, 4 ft. height, and a maximum capacity just under 4000 gal (about 33 kips, or 140 psf average floor load). This diameter was the perfect size to fit on the 15 ft. floor bays, leaving clearance for people to pass between pools built on abutting bays. Four pools were constructed and filled on the ground to store the water between tests.

Floor loads are usually described as uniform pressures over the whole area. The main drawback of water loading with swimming pools is that the ideal loading situation cannot be met: The pool is circular while the bay is square, and the depth of the water changes across the bay as the floor deforms during the column removal test (i.e. “ponding”). Despite these differences, the loading applied in the tests conducted for this research is reported as a smeared uniform pressure load over the affected bays (total water weight divided by floor bay area). However, the companion computer models of the experiments being developed at NIST account

for the real circular loaded area and the ponding effects to more accurately capture the real system behavior.

Water was pumped into the loading pools incrementally using a semi-trash pump with a maximum flow rate of 150 gallons per minute. The pump was placed next to the storage pools with a short intake hose going into a pool and a long outflow hose running up to the floor. The CC test used one pump and one hose. The EC-B and EC-G had two load pools each, so the outflow hose had a "T" junction sending one hose to each pool. The IC test required 4 loading pools, so two pumps were used, each having a "T" in the outflow hose. Volume loaded was measured by monitoring the drawdown of the storage pool(s).

Several other loading methods were considered before the swimming pool plan was chosen. The primary goal of the loading plan was safety: no one could be on the floor placing load while the column removal test was in progress. The secondary goal was to have load that would apply a uniform distributed load on the floor. One plan was to use sandbags that would be lifted in on pallets by crane. The sheer quantity of sandbags needed to deliver 150 psf over four floor bays made the plan unrealistic. Another plan was to have thin slabs of precast concrete that could be placed in a grid on the floor by crane or forklift. The price of all of the slabs as well as the long time required to lift the slabs during testing eliminated this possibility.

It became apparent that pumping water was the only feasible option for fast loading that didn't require people on the floor during the tests. To keep a uniform distributed load while the floor had large displacements would require small cellular containers of water. 55-gallon drums were considered, but did not have enough depth to achieve the loads required. Deeper containers such as agricultural water tanks and livestock water troughs were too expensive. Custom-made plastic-lined plywood containers were also considered as a way to achieve enough depth, but that idea was eliminated because the labor costs to build them would be high and leaks were likely. Another problem with the cellular water container plans was the cost and challenge of distributing water evenly to 16 or more containers without any active flow control except for at the main water pump. Despite the issues of not fully loading the bays and ponding as well as freezing issues during winter testing, loading with water in swimming pools was the only loading method that was not cost-prohibitive, allowed loading without any people on the floor during the tests, and could consistently distribute even volumes of water between containers.

2.4.2 TEST PROCEDURE

The water was loaded onto the floor incrementally so that there would be multiple discrete equilibrium points. The loaded bays (those adjacent to the removed column) were first pre-loaded with a few inches of water in the pools. This pre-load stabilized the pools, which are quite flimsy when completely empty and allowed water to be pumped at a consistent rate into the pools after column removal.

Next, a crane held the upper section of the removal column so that the lower column section could be removed. After the lower column section was removed, the crane lowered the floor to the first equilibrium point, defined as the point where all the load from the pre-load and the self-weight of the floor was resisted by the floor and the crane load went to zero. Next, the crane held the floor in that position as the next water load increment (generally 5 psf) was pumped into the pools (Figure 2.18). Then the crane slowly lowered the floor again to the next equilibrium point. This incremental loading procedure was repeated until the floor could not carry more load and thus the crane load could not be reduced to zero. This point marked the stage at which the floor no longer had the capacity to carry the applied load. In most tests, the crane was lowered further after the floor was past its capacity so that additional structural damage could be observed.

Figure 2.18 Crane Supporting Removed Column During EC-B Test

After failure, the crane lifted the floor back to horizontal and the lower section of the removed column was replaced. Temporary shoring was placed under the floor for safety, even though the floor had adequate stability once the removed column was replaced. The water from the loading pools was then pumped back into the storage pools. This procedure was used for the first three tests (corner and edge column removals), but the last test (interior column removal) was conducted using a different method, as described in section 3.4.1 .

The DAQ continued running from the very beginning of pre-loading to the end of pool emptying after the test was complete so that beam and girder strains and column loads could be tracked through the whole loading, testing, and unloading process. Along with instrument data collection, video (with sound) and time-lapse photography recordings were made.

2.4.3 ANCILLARY TESTING

Ancillary tests were performed to determine the material properties of the steel and concrete used as well as to gain a better understanding of the interaction between the concrete slab and metal decking. Compression tests were performed for the footing concrete after 28 days, compression tests and split cylinder tests were performed on the floor slab concrete after 3, 7, and 28 days as well as on the same day as every column removal test. Steel coupon tests measured yield stress and ultimate stress for the flanges and webs of all W-sections as well as the decking and welded wire fabric. The steel coupons were cut from the drop sections of the steel order. A summary of ancillary test results is in Table 2.1 and detailed test results are tabulated in Appendix A.

Table 2.1 Ancillary Test Results

Steel Material Properties

Steel Section	Mean Yield Stress (ksi)	Mean Ultimate Stress (ksi)
A992 W-Sections		
W6x9 Flange	52.6	76.8
W6x9 Web	53.0	76.4
W8x10 Flange	48.2	63.9
W8x10 Web	51.0	65.1
W8x24 Flange	47.6	64.8
W8x24 Web	51.6	66.9
Other Steel Sections		
Decking	45.9	59.4
WWF	N/A	98.6

Deck Concrete Material Properties

Date	Test	Mean Compressive Strength, f'_c (psi)	Mean Tensile Strength, f_t (psi)
6/24/13	**3 Day**	2867	367
6/28/13	**7 Day**	3717	419
7/19/13	**28 Day**	4821	504
11/15/13	**CC Test**	4814	458
12/6/13	**EC-B Test**	4741	428
12/13/13	**EC-G Test**	4973	539
3/21/14	**IC Test**	4461	419

Footing Concrete Material Properties

Date	Test	Mean Compressive Strength, f'_c (psi)
5/29/13	**28 Day**	4812

Non-destructive testing (NDT) of the floor slab was performed to determine the level of bonding between the concrete and metal decking and to examine the potential effect of deck defects in the failure of the floor during column removal tests. Anna Molins Estellés (2014), a student who studied with John Popovics' NDT research group at UIUC Civil Engineering, first calibrated two different testing apparatuses on a concrete test slab in the lab. The Nitto Hammer determined material stiffness and helped to detect defects in the concrete by measuring active (ZA) and reactive (ZR) impedance. Impulse-response testing provided a more detailed look at the presence of defects in the concrete due to material issues or delamination within the concrete or at the interface between the concrete and the deformed steel decking.

Estellés then tested the floor bay loaded in the CC test (A4 corner) before and after the column removal test. She first tested a 22 x 22 ft. area (15 ft. of the corner bay plus 7 ft. into the adjacent bays) with the Nitto Hammer to ascertain the quality of the concrete placement. The difference in active impedance in different areas was small but noticeable, implying slightly different concrete conditions in different mixing trucks. She then selected two 2-ft. squares on the corner bay, one that the Nitto Hammer indicated was very good quality concrete placement and one that appeared to have some defects, and did a more detailed test with impulse-response. She concluded that there were a few places with minor defects. The defects were not from debonding, but Estellés predicted that these locations were nevertheless the most at risk for debonding and delaminating during the column removal tests.

After the CC test concluded, Estellés again tested the 22 ft. square with Nitto Hammer and the small squares with impulse-response. Her predictions of damage proved correct: though the entire floor bay had debonded, the previously defective area suffered more damage than the area that had been free of defects. Her findings suggest that if concrete floor slabs are placed with higher quality and fewer defects, the concrete could resist more load before it cracks and fails, perhaps slightly increasing the capacity of the floor after column removal.

CHAPTER 3 - EXPERIMENTAL RESULTS

3.1 SUMMARY OF DATA ANALYSIS TECHNIQUES

The raw data was collected using Labview on a National Instruments data acquisition (DAQ) chassis, and subsequently processed using MATLAB. The strain gauge data for the linear strain gauges, rosettes, and strain gauge bridges was noisy and required filtering. The filter used was a standard running average ('filter' function in MATLAB) of 20 to 200 samples (4 to 40 seconds) depending on the quality of the particular data set. The tests ran slowly enough that a 40 second average could still capture the overall trends in behavior for the specimen components being measured. The string pot and inclinometer data was clean and did not require filtering.

As previously described, the DAQ began data collection before the pre-load stage. However, the figures presented in this thesis generally have a datum set just prior to column removal. The strain plots are presented as change in strain from the datum instead of absolute strain so that the relative difference and changes in strain over time and between components and tests could be easily seen. The datum for the column load plots is the first equilibrium of each test.

Markers on the plot lines of the figures denote hold points in the floor displacement. Generally, these are equilibrium points, but the last few markers on each plot are points when the crane held the floor in place but there was no equilibrium.

3.2 CORNER COLUMN REMOVAL TEST

3.2.1 SUMMARY

The corner column (CC) test was conducted on November 13, 2013, and lasted approximately one hour, starting at 10:00 AM CST. Only one equilibrium point was reached (Figure 3.1) and the floor could not hold the first additional load increment. The floor resisted much less load than expected and as a result, the initial water load should ideally have been much smaller so that multiple equilibrium points could have been obtained leading up to the collapse load. After the floor was beyond capacity, the crane let the floor displace more so its behavior could be observed through very large deformation. Figure 3.2 shows the displacement of the corner column throughout the test. The first plateau is the hold at the first equilibrium. The two subsequent holds were post-failure and equilibrium was not achieved. The initial water load

was 9.75 in. (60 psf total) and the first and only load increment of 3 in. of water added 10 psf for a final load of 70 psf.

Figure 3.1 CC Test at First Equilibrium (8.25 in. Displacement, 60 psf)

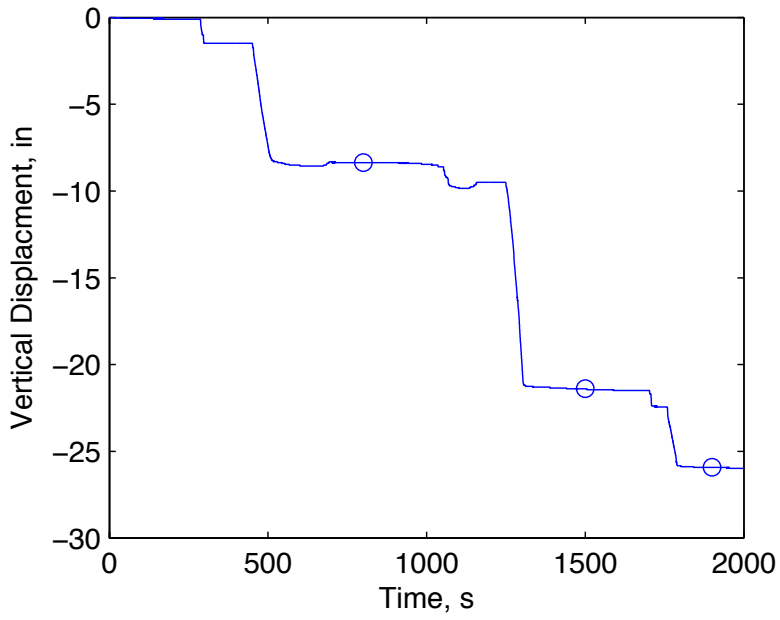

Figure 3.2 CC Test Removed Column Displacement

3.2.2 CC MEMBER, CONNECTION, AND FLOOR ROTATION

Most of the deformation in the corner bay was from the composite floor slab bending and eventually cracking. The beams and girders remained relatively rigid as they rotated with the floor. Refer to Figure 3.3 for the inclinometer arrangement. Figure 3.4a and Figure 3.4b show that the rotations measured along the length of the spandrel beam and spandrel girder were relatively consistent (within one degree), showing that the member rotations were nominally rigid. The rotations of the floor along the diagonal from B3 to the corner, A4, was not rigid. Rotations in both the north-south axis and the east-west axis were smaller towards the interior corner of the floor bay (Figure 3.4c) than closer to the corner (Figure 3.4d). These different rotations are consistent with cantilever bending of the floor, where rotation is greater towards the tip.

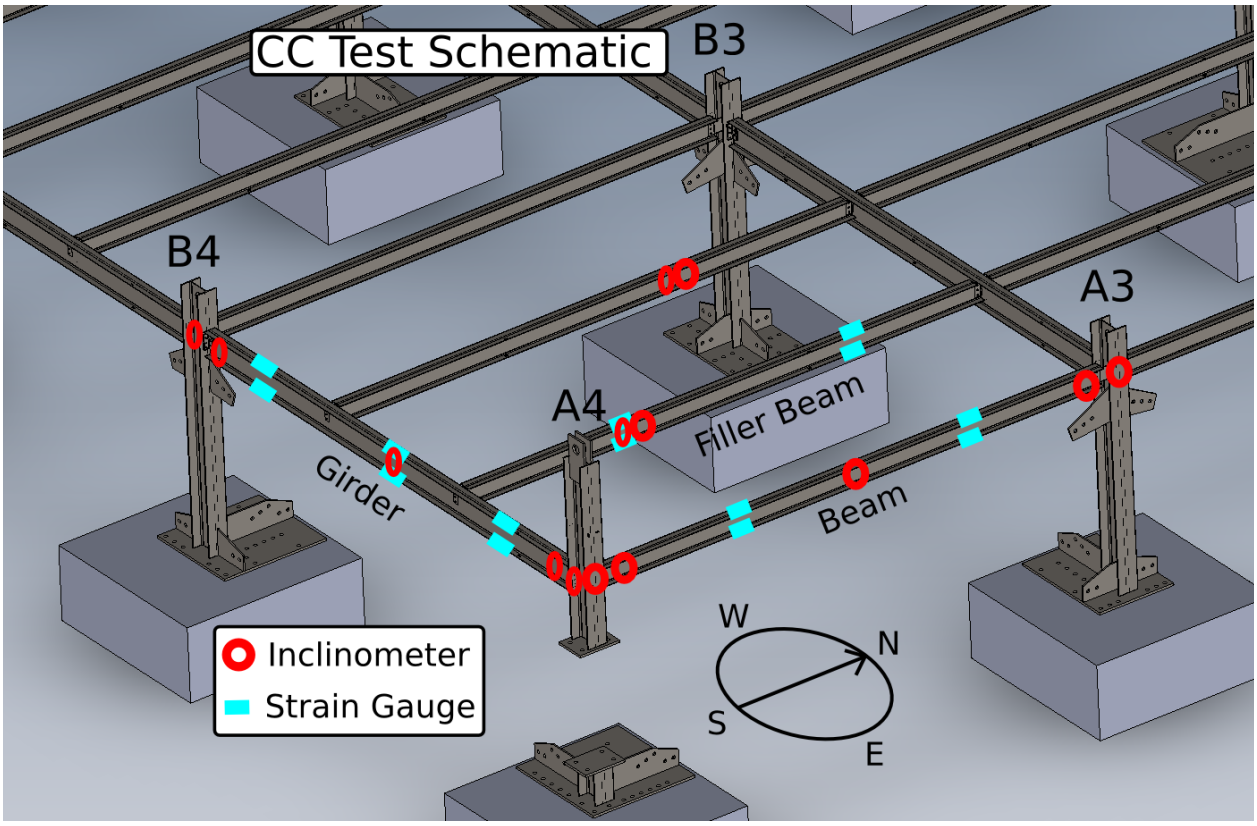

Figure 3.3 CC Test Inclinometer and Strain Gauge Placement

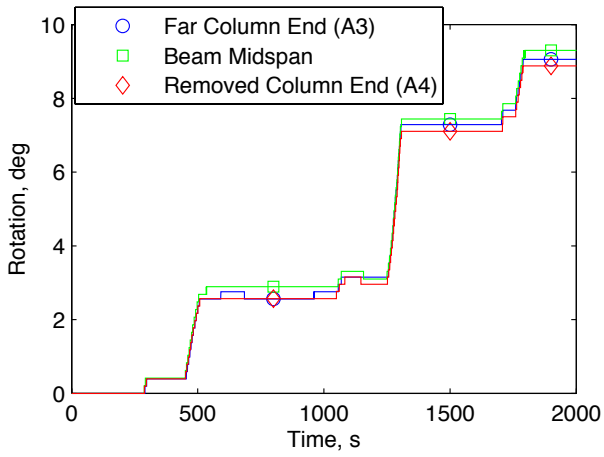

(a) Beam Rotation

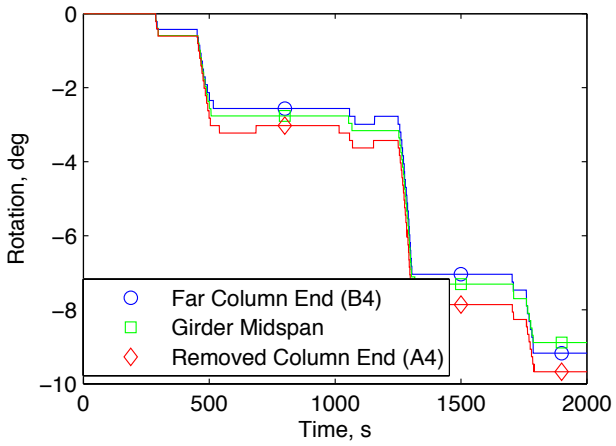

(b) Girder Rotation

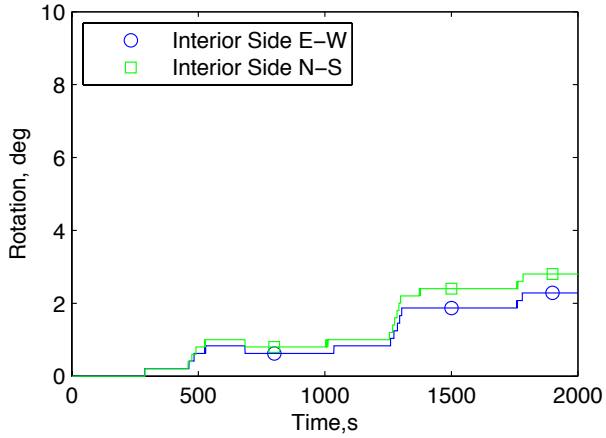

(c) B3-A4 Diagonal Interior Side

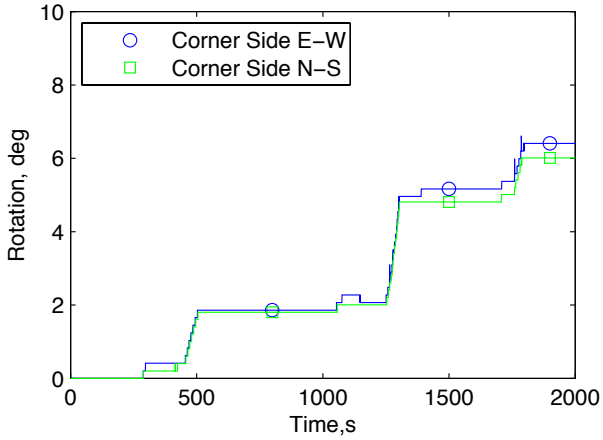

(d) B3-A4 Diagonal Corner Side

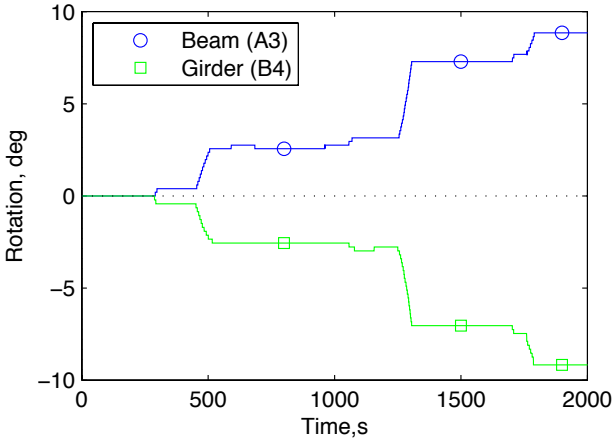

(e) Connection Rotations at Far Columns

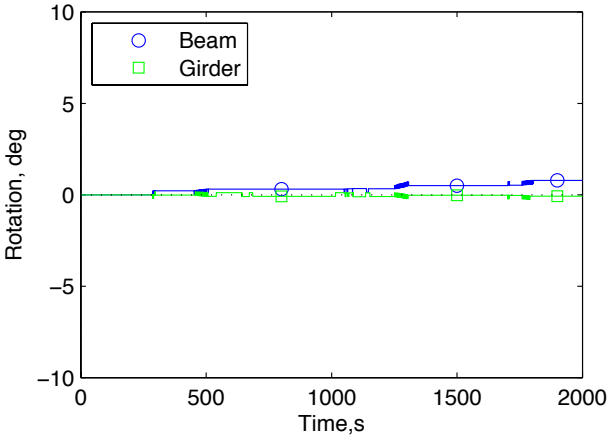

(f) Connection Rotations at A4

Figure 3.4 CC Test Rotation of Floor Members, Slab, and Connections

Since the beam and girder remained essentially rigid, the deformation occurred in the connections at A3 and B4. Columns A3 and B4 had negligible rotation. The beam-to-column connection at A3 (Figure 3.5a) was a shear tab with three bolts. At first, the bolts elongated the bolt holes in the shear tab, and then the bottom bolt sheared during the last lowering of the removed column corner. Figure 3.4e shows the connection rotations at the far columns, A3 and B4. The girder-to-column connection at B4 (Figure 3.5b) was a bolted double-angle. Most of the deformation at B4 was from prying action in the double angle. With enough displacement of the removed column corner of the bay, the top bolt in the connection sheared. The girder-to-column connection acquired additional stiffness when the bottom flange of the girder began to bear on the flange of the column as the girder rotation increased.

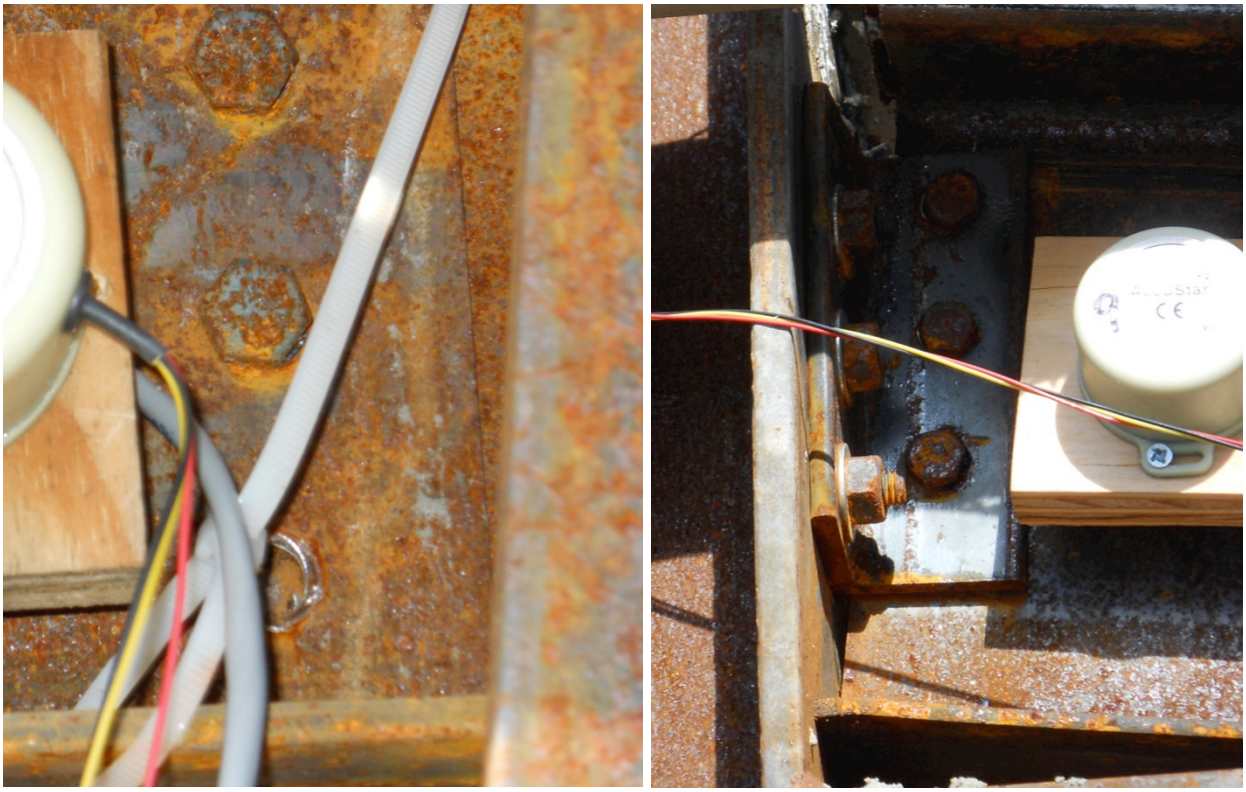

(a) Bolt Shear in Beam Connection at A3 **(b) Prying Action and Flange Bearing at B4**

Figure 3.5 CC Test Deformation and Failure of Connections

One of the limitations of the test specimen was the lack of multiple stories. An actual multi-story building would have columns extending above the floor being tested, and the columns would be braced by the upper floors. In the test scenario, the column connected to the crane was free to rotate in this single story test specimen since there was no column bracing from

other floors above. There was almost no relative rotation between the beam or girder and the corner column stub (Figure 3.4f), indicating that the column rotated with the beam and girder. This is clearly illustrated in Figure 3.6.

Figure 3.6 CC Test Corner Column Rotated Freely with the Beam and Girder

3.2.3 CC MEMBER AND FLOOR STRAINS

Strain data was collected from uniaxial gauges on the flanges of the spandrel beam and spandrel girder and a filler beam, as well as from strain rosettes on the galvanized steel decking and embedment gauges in the floor slab. The plots of strain vs. time in Figure 3.7 show change in percent strain with the beginning of the test being the datum. Refer to Figure 3.3 for the arrangement of the beam and girder strain gauges. Although many gauges did not provide useful data, the data that was collected from the beam, filler beam, and slab, further support the results from the inclinometer data. Figure 3.7a shows that the spandrel beam had a small magnitude of strain change, indicating it remained relatively rigid as the inclinometers suggested. The filler

beam, with single-angle connections, had more bending, indicated by greater magnitudes of strain change. Figure 3.7b shows the concrete strain along the diagonal and in the east-west direction. Tension increased in the slab as the corner displaced throughout the test. The cantilever load capacity of the non-composite girder and filler beams was not enough to extend the overall floor capacity after the concrete cracked.

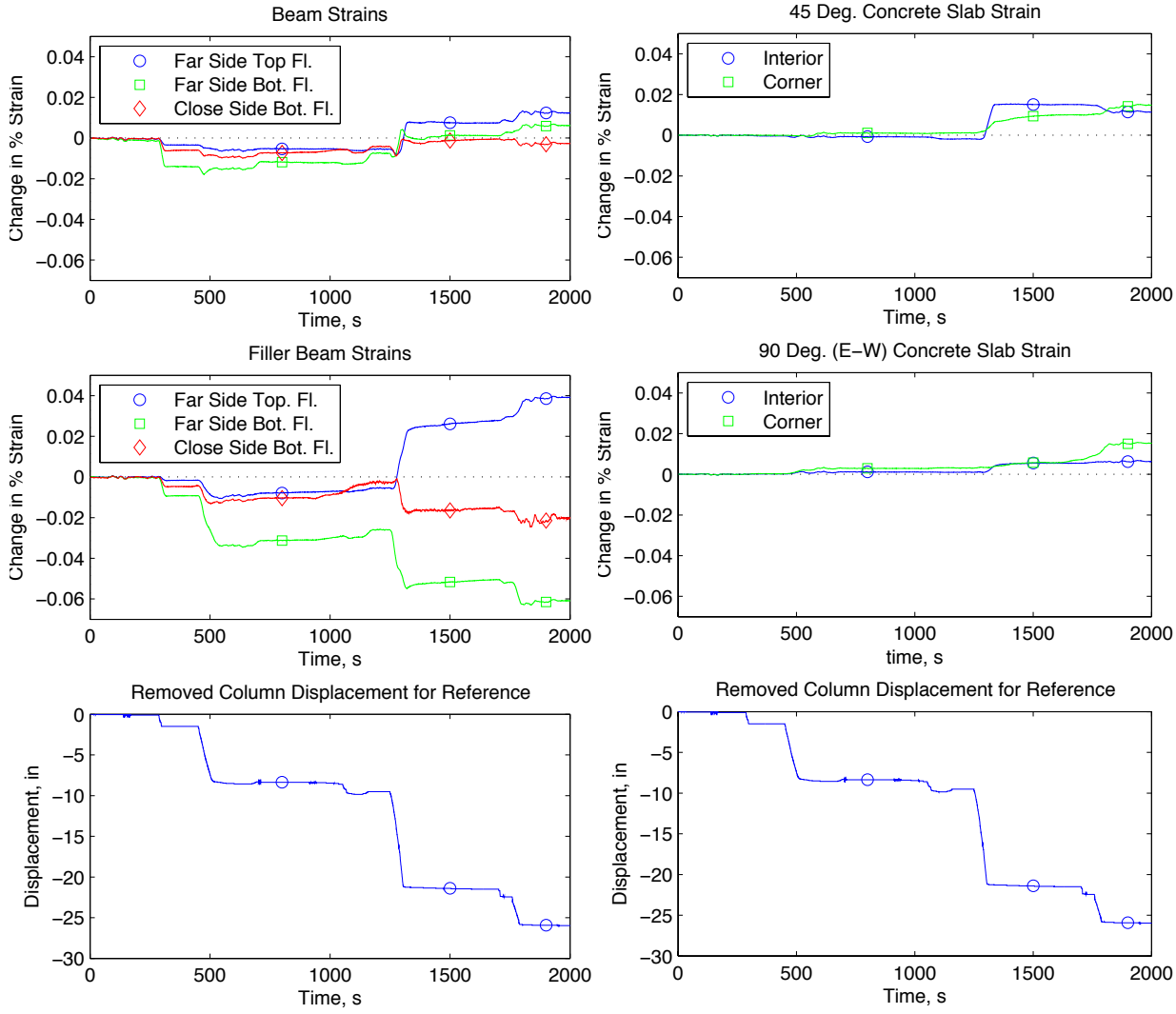

(a) Beam Strain **(b) Floor Slab Strain**

Figure 3.7 CC Test Strains

3.3 EDGE COLUMN REMOVAL TESTS

3.3.1 SUMMARY

Two edge column removal tests were performed: one at A2 with spandrel beams (EC-B) and the other at C4 with spandrel girders (EC-G). The EC-B test was performed on December 4, 2013, beginning at 9:00 AM CST and lasting 1.5 hours. The EC-G test was performed on December 11, 2013, beginning at 9:30 AM CST and lasting 1.5 hours. The initial loads of dead weight plus water were 42 psf and 43 psf respectively. The load increments were 5 psf. The two floor sections failed at almost identical loads of 88 and 89 psf, but the displacements and ductility were quite different. Figure 3.8 shows the load vs. displacement curves for the edge column tests.

While both failed at essentially the same load, the EC-B test displayed more ductility. In the initial load increments before any concrete cracked, both floor sections had the same stiffness (defined based on vertical load-deflection behavior). At around 5 in. of displacement, the concrete slab cracked in the EC-B test, causing much larger subsequent displacements. The floor continued to resist load up to 83 psf (Figure 3.9a) and failed with 88 psf. (Figure 3.9b)

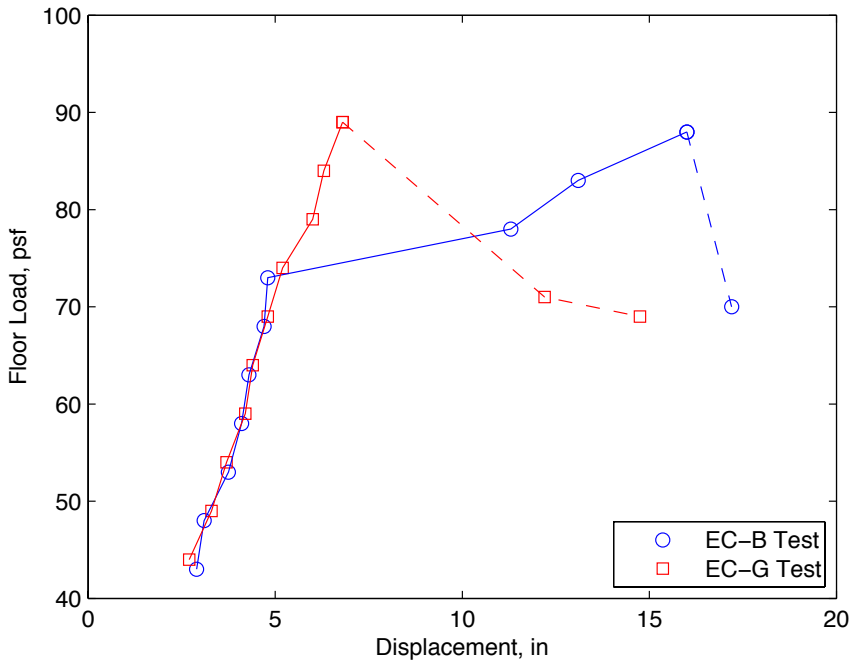

Figure 3.8 Edge Column Tests Floor Load vs. Removed Column Displacement

The final equilibrium for the EC-G floor bays was 84 psf (Figure 3.10a). The floor failed at 89 psf when the concrete slab cracked and the steel framing failed simultaneously (Figure

3.10b), as illustrated by the lack of ductility in the EC-G plot in the figure. The dashed lines in Figure 3.8 indicate the estimated post-failure reduction in floor load as the crane carried more load with increased displacement.

(a) Final Equilibrium (13 in. Displacement, 83 psf)

(b) Post-Failure Deformation (16 in. Displacement, 88 psf)

Figure 3.9 EC-B Test Failure

(a) Final Equilibrium (6.25 in. Displacement, 84 psf)

(b) Post-Failure Deformation (6.75 in. Displacement, 89 psf)

Figure 3.10 EC-G Test Failure

3.3.2 EC-B RESULTS

3.3.2.1 EC-B COLUMN LOADS

With a column removed, it is important to observe how the floor load redistributes to the remaining intact columns. Wheatstone bridges, or full strain gauge bridges (SGBs), were built with four linear strain gauges on the columns and diagonal braces. The Wheatstone bridges recorded strain in the columns and braces with bending and temperature effects being negated by the configuration of the strain gauges. Strain was converted to load given the strain, Young's Modulus for steel (29000 ksi), and the cross-sectional area of the columns and double-angle braces. Column load was calculated as the sum of the load in the column and the vertical component of brace loads at the column location.

Figure 3.11a illustrates that all of the column loads grew at the same rate with the exception of column B2 at the supported end of the girder. To validate the accuracy of the gauges, the sum of the SGBs on columns and braces supporting the loaded bays were compared to the total applied load, dead load + water load, which is known. Figure 3.11b shows this comparison. For the EC-B test, the sum of measured column loads divided by floor area, to produce average floor load, matched the actual floor load with an error less than 5 psf. The close tracking of measured and actual load validates the accuracy of the SGBs, allowing further use of the data in analysis.

Before column removal, the central edge column to be removed (A2), the central interior column (B2), the corner edge columns (A1+A3), and the corner interior columns (B1+B3) would each take nominally 25% of the total load. (Note that the SGB at A1 was broken, so it was assumed to be equal to the SGB at A3.) Knowing that these column loads would be equal under normal circumstances, Figure 3.12 shows how the loads were redistributed when column A2 was removed. The figure shows the redistribution of total load, in percent, taken by each group of columns. The redistribution took time to settle in the figure because the noise in the SGB data had larger effects when the total load was smaller (as seen in the first 500 seconds of data in Figure 3.11a). Once the data settled, the redistribution of load was roughly constant throughout the test as more load was added. The interior middle column at B2, where the girder is connected, took 50% of the load, while the columns on the corners of the loaded bays took only 25% per pair. This distribution indicates that the girder, acting primarily as a cantilever, redistributed much more load than the spandrel beams and filler beams acting as ties.

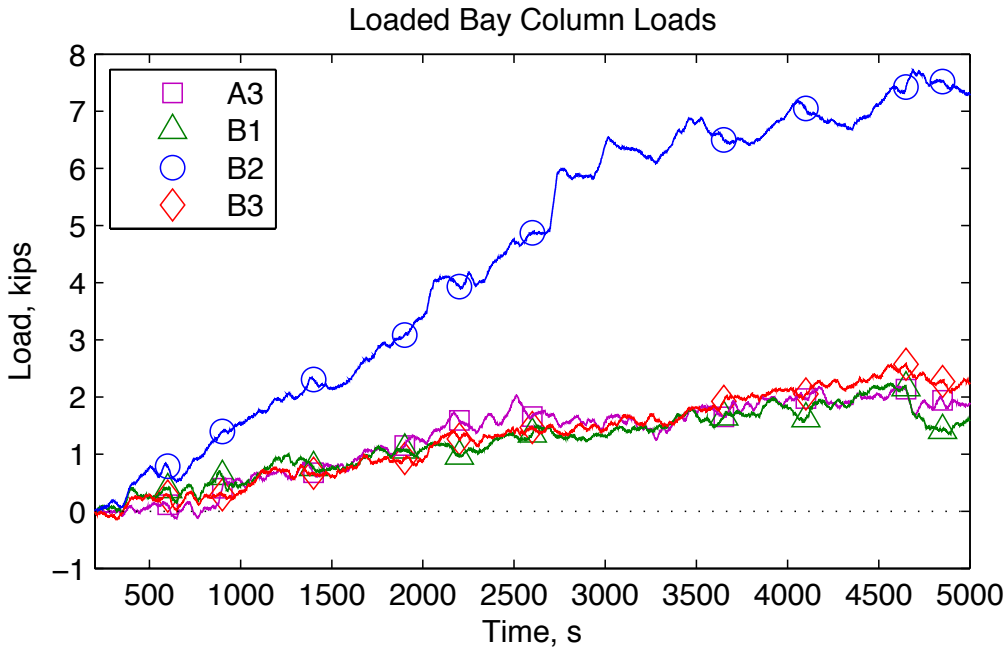

(a) Increase in Individual Column Loads After First Equilibrium

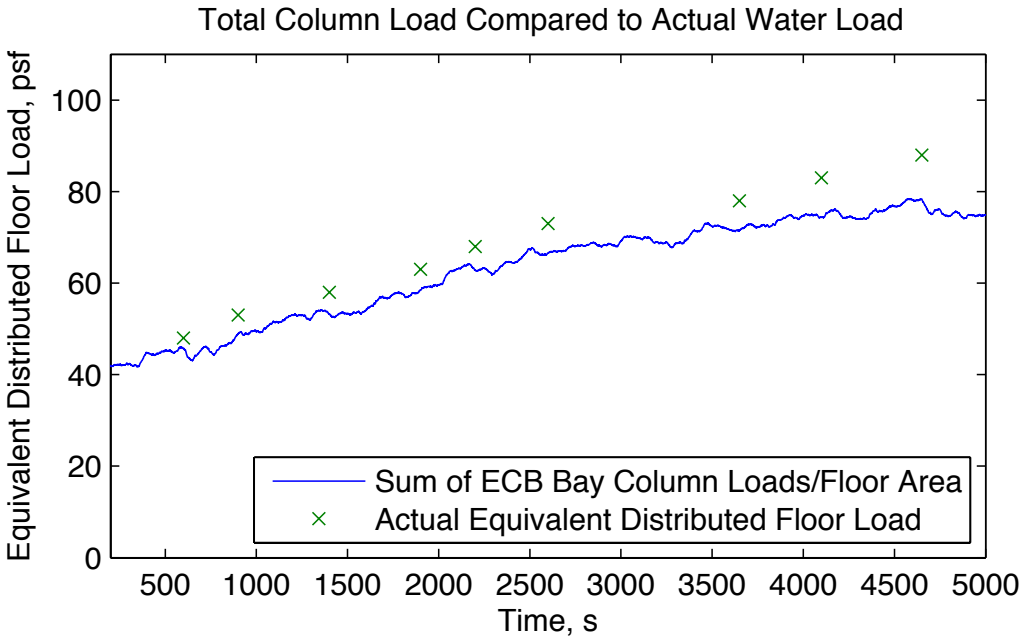

(b) Comparison of Total Measured Column Load and Actual Water Load

Figure 3.11 EC-B Test Loaded Bay Column Loads

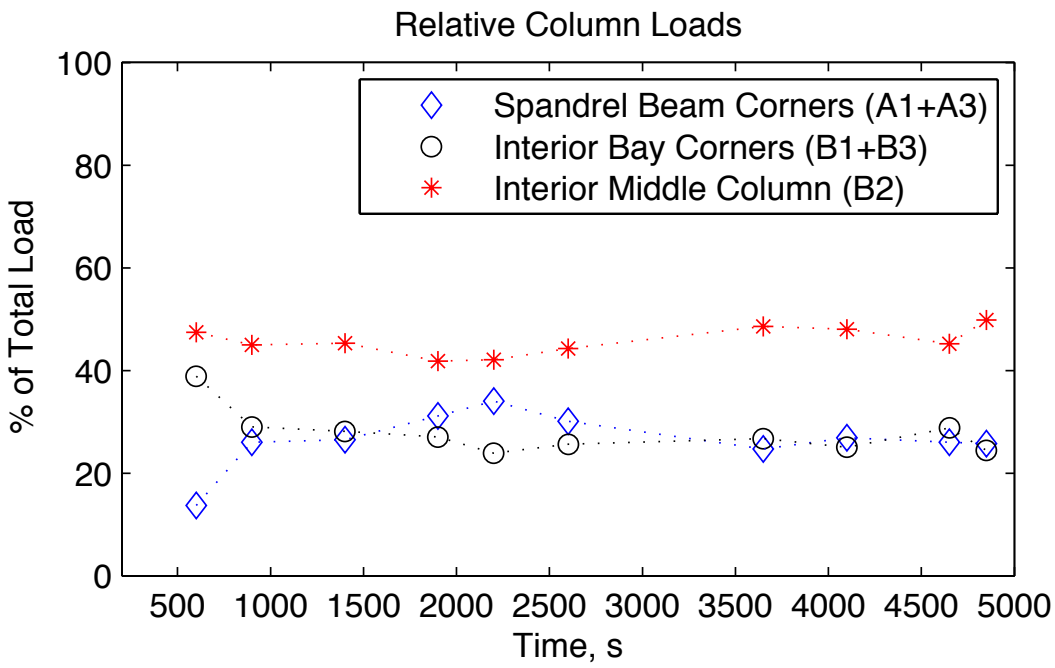

Figure 3.12 EC-B Test Relative Distribution of Load to Different Column Locations

3.3.2.2 EC-B MEMBER AND CONNECTION ROTATION

The two domains of displacement in the EC-B test, a stiff floor with small displacements before concrete cracking and a flexible ductile floor with large displacements after concrete cracking, are seen throughout the rotation data results provided by the inclinometers. Refer to Figure 3.13 for the arrangement of the inclinometers. The cracking, which occurred around 2800 seconds into the test, caused the sharp increase in displacements and rotations seen in Figure 3.14. Figure 3.14a shows the removed column displacement over time for reference and the transition from small to large displacements is clearly seen.

In the first domain of deformation, the girder (Figure 3.14b) rotated rigidly as it resisted load with the composite steel-concrete section still largely intact and carrying tension in the upper portion of the section (steel deck, welded wire fabric, and concrete). This type of negative moment resistance has been observed in prior dynamic numerical simulations of full-building response to column loss scenarios (Hoffman and Fahnestock, 2011). After the concrete cracked and the composite action was lost, the upper portion of the section could no longer resist much tension. Thus, the steel girder accounted for all of the cantilever action along the girder line. Greater rotations at the removed column end than the far end indicate cantilever flexure in the girder.

The shear tab beam-to-column connections resisted little moment so the beams did not develop any appreciable cantilever action. The spandrel beams rotated rigidly throughout the test, as seen in Figure 3.14c and Figure 3.14d. The sharp increase in rotation here is another indicator of the second, ductile, domain of the EC-B test deformation.

The shear tab beam-to-column connections rotated more than the double-angle girder-to-column connections. At the far end of the members away from the removed column, Figure 3.14e shows the greater rotation in the beam connections. Figure 3.14f shows the same thing for the removed column connections, but also shows that most of the connection rotation in the beams was concentrated on the north beam. By late in the test, the upper section of the removed column had rotated out and to the north so that the connections remained relatively rigid except for the north beam connection. In an actual multi-story building, upper floors above the lost column would brace the intact sections of column, keeping it essentially vertical. In this test case, the lack of lateral bracing in the column left it free to rotate, causing all of the connection deformation to be in one connection. (Figure 3.15)

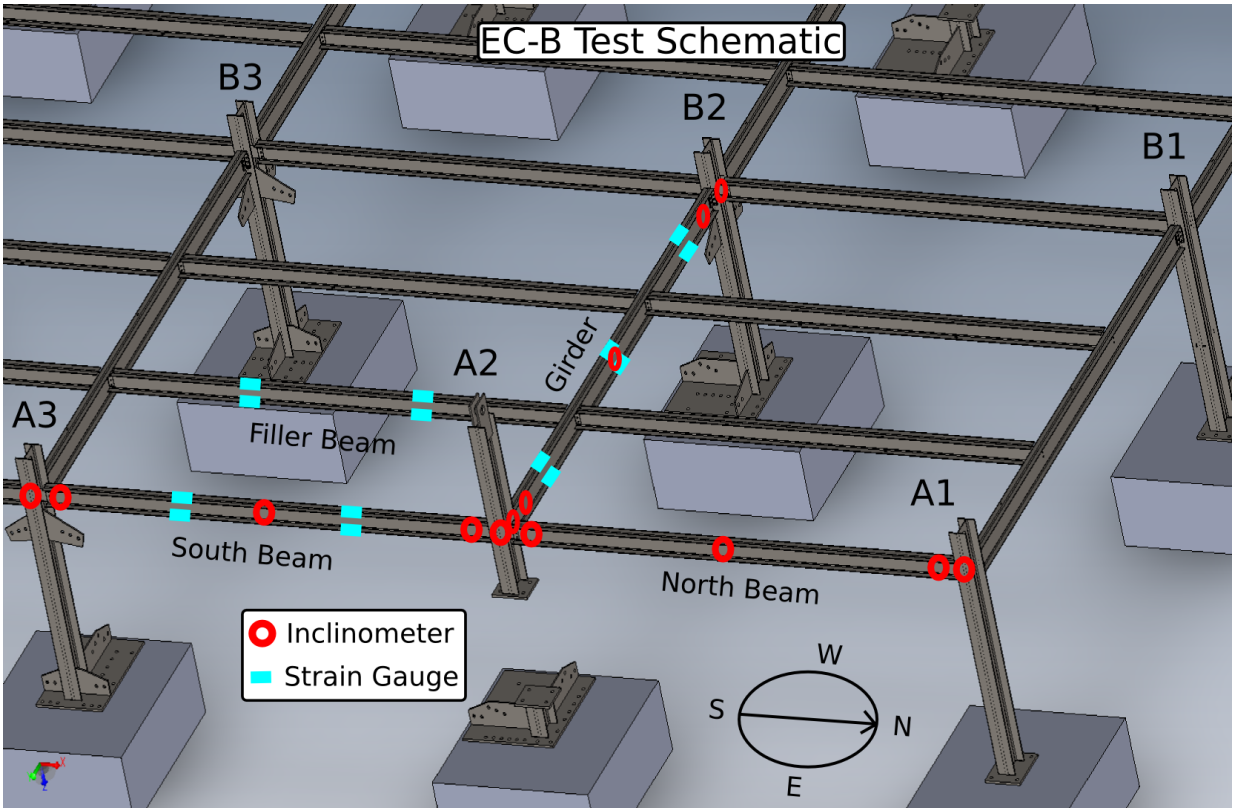

Figure 3.13 EC-B Test Inclinometer and Strain Gauge Placement

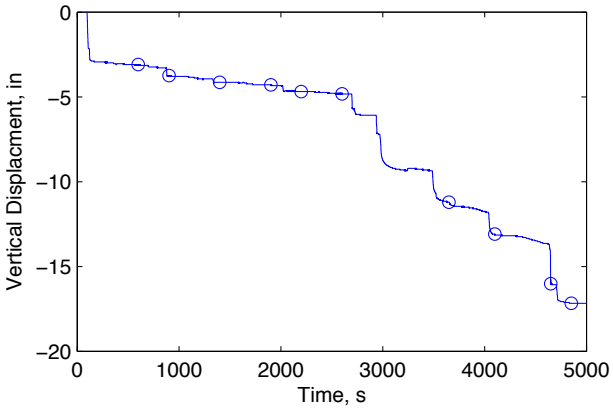

(a) Removed Column Displacement

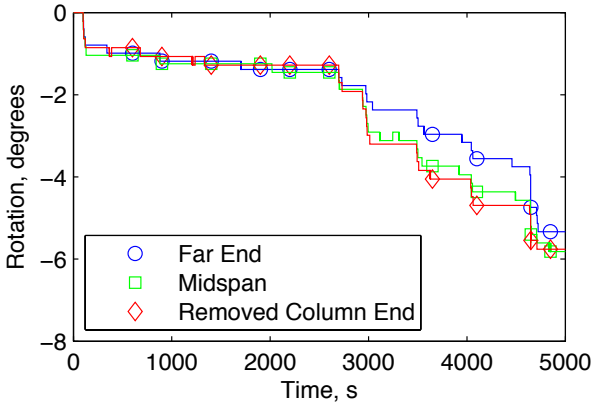

(b) Girder Rotation

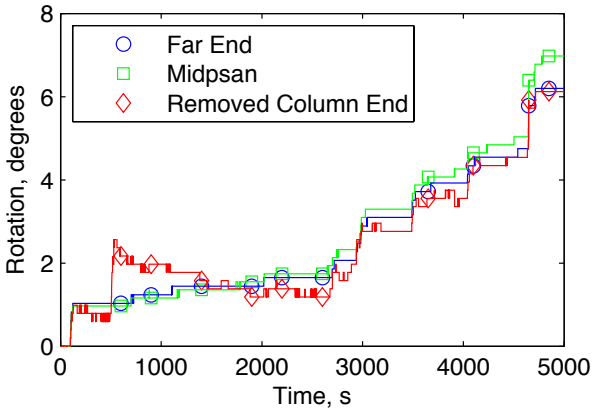

(c) North Beam Rotation

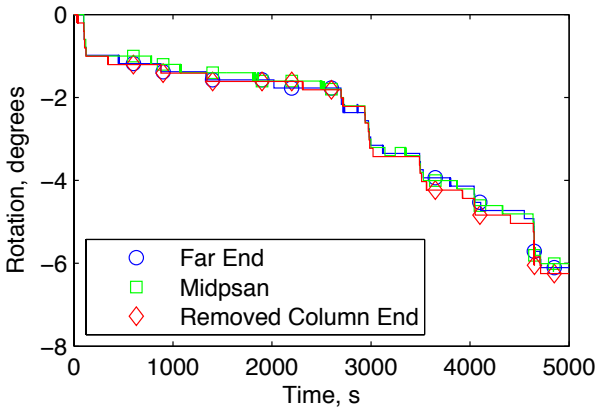

(d) South Beam Rotation

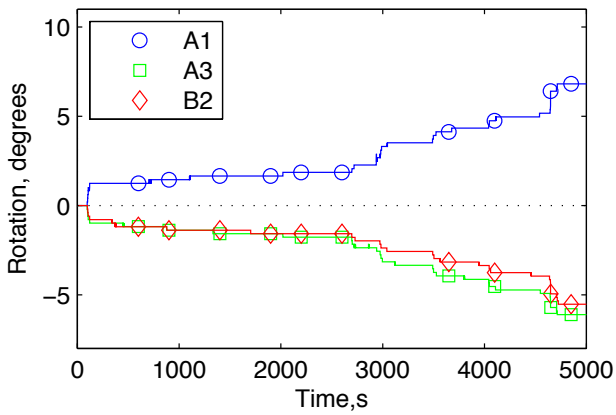

(e) Connection Rotations at Far Columns

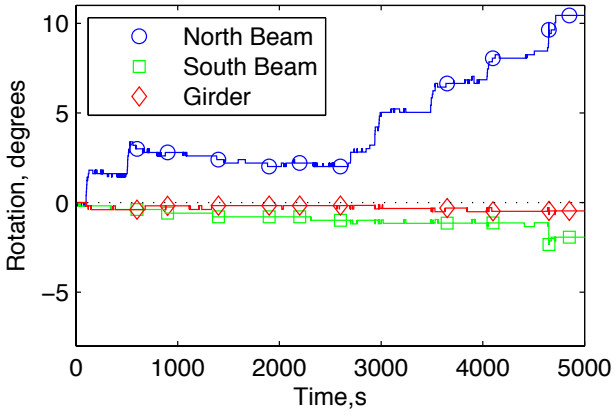

(f) Connection Rotations at A2

Figure 3.14 EC-B Test Removed Column Displacement and Member and Connection Rotations


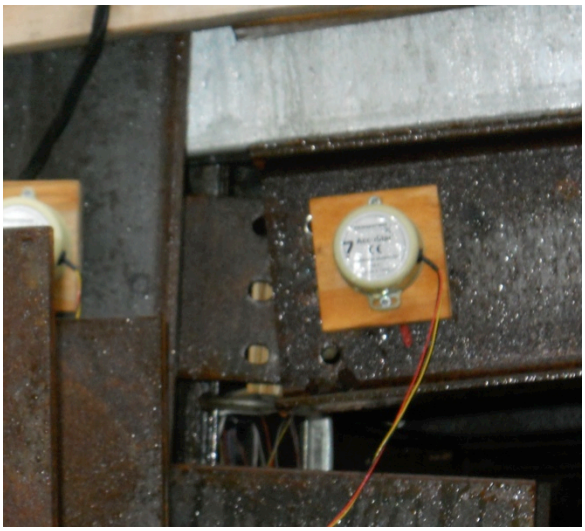

(a) Upper Column Section Rotation **(b) North Beam Connection Deformation**

Figure 3.15 EC-B Test Removed Column Rotation at A2

3.3.2.3 EC-B CONNECTION EXTENSIONS

Connection extensions in the EC-B test further illustrate the unequal distribution of connection deformation at the removed column. Connection extensions were measured using string potentiometers (string pots) attached to the flexural members and the columns. The data was processed to eliminate the extension of the string pots caused by the rotation of the connection. Assuming that the centroid of the beam was the center of rotation, the following equation was used to calculate connection extension:

$$Connection\ Extension = S - w * \tan(\theta)$$

Where:

S = String pot displacement data

w = Offset distance from beam centroid to string

θ = Connection rotation (in degrees)

Figure 3.16 shows the connection extensions at the removed column (a) and the far columns (b). The magnitudes of the extensions are very small for all connections except the north-beam-to-removed-column connection, which can be seen in Figure 3.15b.

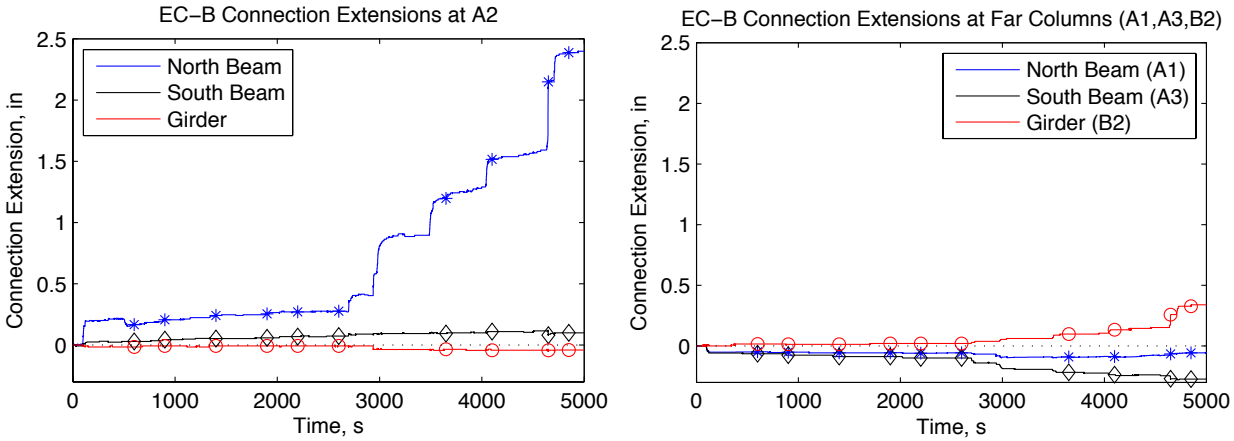

(a) Connections at Removed Column (A2) **(b) Connections at Adjacent Columns**

Figure 3.16 EC-B Test Connection Extensions

3.3.2.4 EC-B MEMBER STRAINS

Along with the rotation measurements, the strain recordings in the beams and girders of the EC-B test show how deformation increased and floor behavior shifted when the concrete floor slab cracked. The strain diagrams in Figure 3.17 show change in percent strain with the beginning of the test being the datum. Refer to Figure 3.13 for the locations of the strain gauges. Before the cracking, the beams and girders were composite with increased tension capacity at the top of the section in the steel deck, welded wire fabric and concrete. When the concrete cracked and the composite action was lost, the neutral axis of the beams and girders shifted down so that, like a typical non-composite cantilever, the top flange was in tension and the bottom was in compression. Figure 3.17a shows the change in strain in the girder flanges from the beginning of the test. The magnitude of strain jumped up just before 3000 s when the concrete cracked. There is less of a clear pattern in the beam and filler beam strains (Figure 3.17b) because the beams were not acting as cantilevers, but provided strength as ties with catenary action.

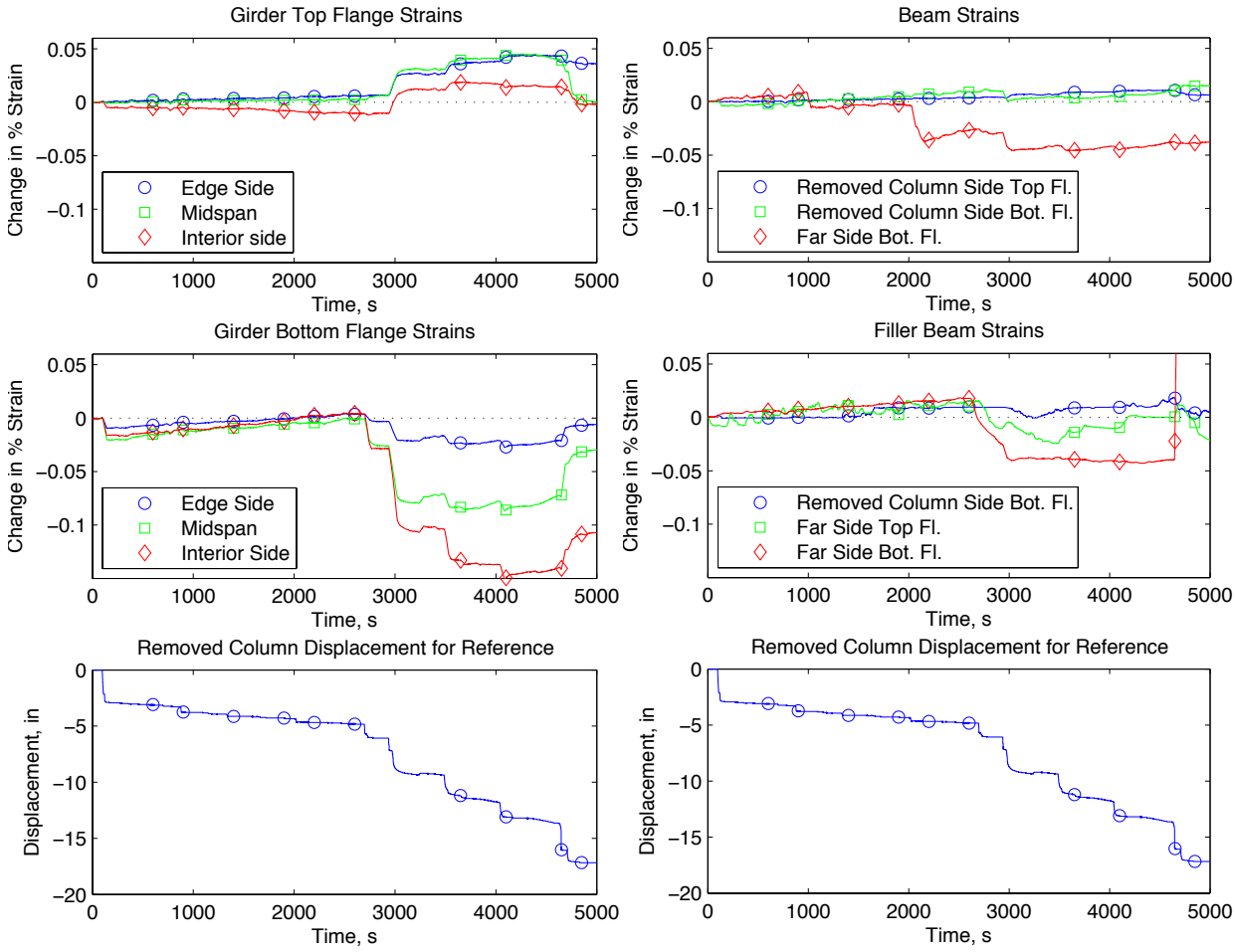

(a) Girder Strains **(b) Beam and Filler Beam Strains**

Figure 3.17 EC-B Test Beam and Girder Strains

3.3.3 EC-G RESULTS

3.3.3.1 EC-G COLUMN LOADS

Column loads were again measured with strain gauge bridges (SGBs). Figure 3.18a shows the individual loads for the columns supporting the loaded bays. Columns B4 and D4 grew to the greatest load with C3 close behind. (Note that the SGB at B4 was broken, so it was assumed to be equal to the SGB at D4.) Like with the EC-B test, column loads from the SGBs were validated by comparison to the actual dead load + water load. Figure 3.18b shows the reasonable agreement between the SGBs and the applied load.

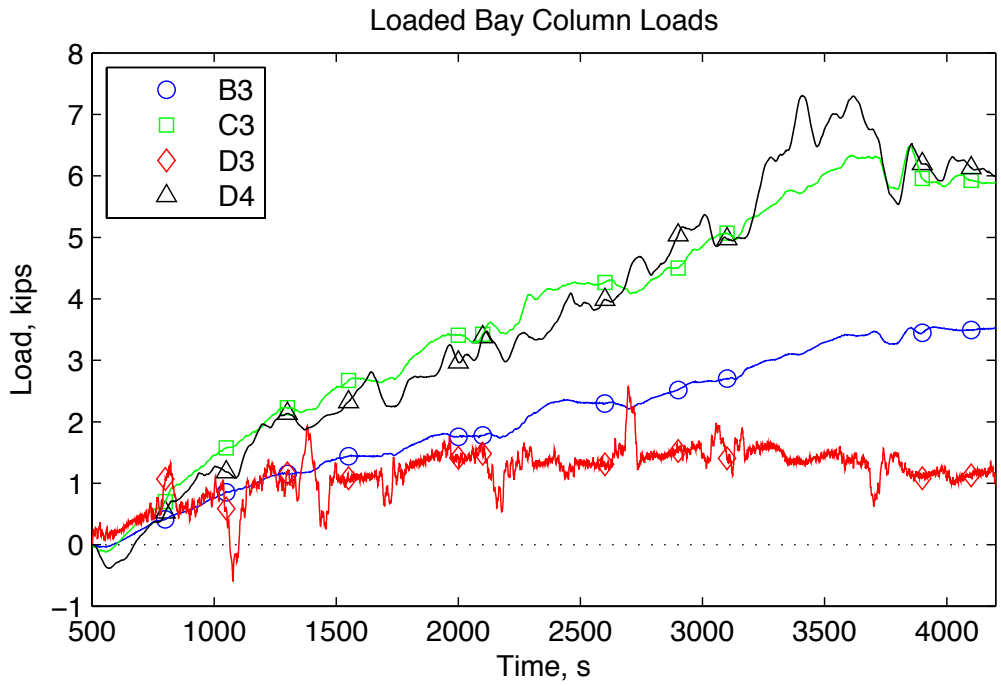

(a) Increase in Individual Column Loads After First Equilibrium

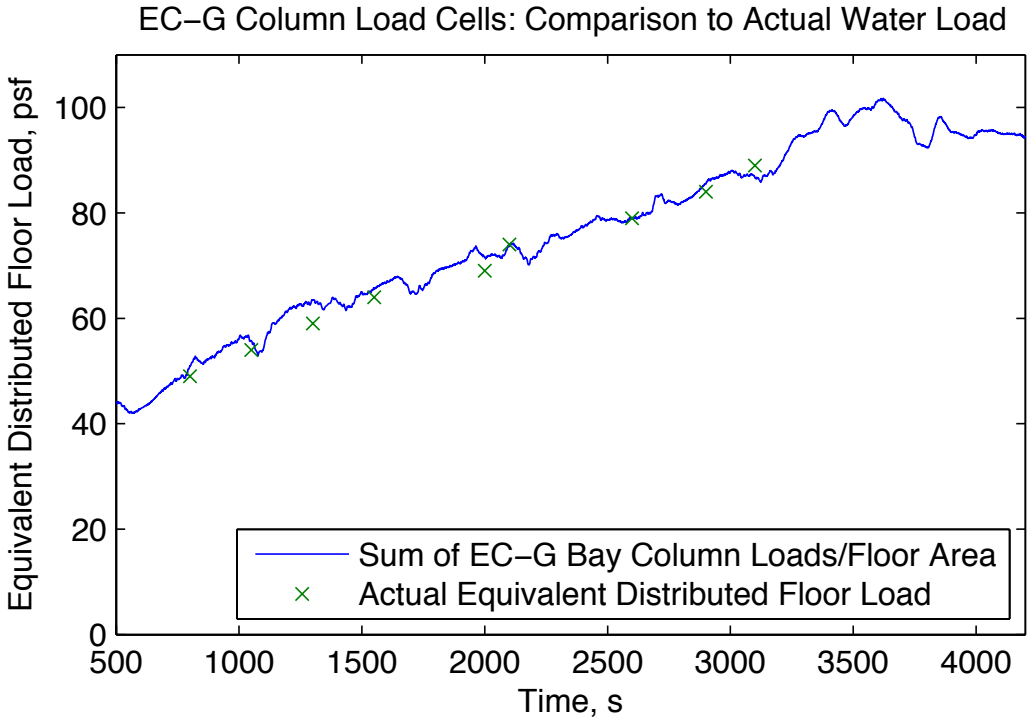

(b) Comparison of Total Measured Column Load and Actual Water Load

Figure 3.18 EC-G Test Loaded Bay Column Loads

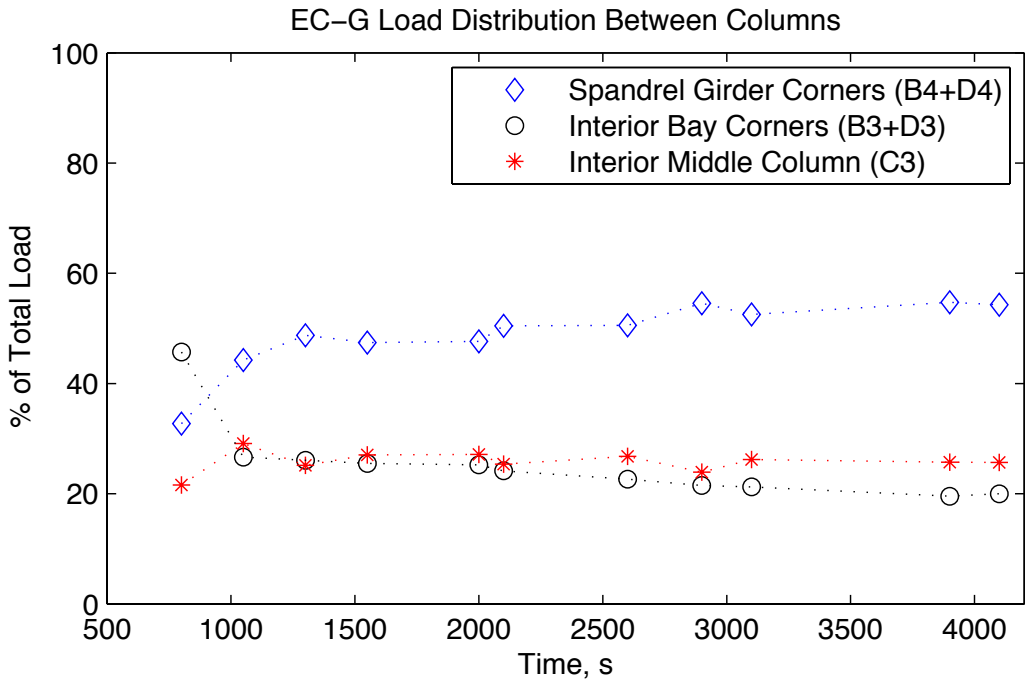

Figure 3.19 EC-G Test Relative Distribution of Load to Different Column Locations

Next, it is important to understand how the loads redistributed when the column was removed. Before column removal, the central edge column to be removed (C4), the central interior column (C3), the corner edge columns (B4+D4), and the corner interior columns (B3+D3) would each take nominally 25% of the total load. It took some time for the load redistribution to settle after the column was removed at approximately 500 seconds. It can be seen in Figure 3.19 that once the load redistribution settled at approximately 1000 seconds the entire load taken by the removed column shifted to the spandrel girder end columns, B4 and D4. Those columns increased to 50% and beyond of the total load. Meanwhile, the other sets of columns remained at 25% and actually decreased in load proportion as the test went on. The edge corner columns took a slightly larger portion of the load because the spandrel girders acted as both ties and cantilevers in this configuration.

3.3.3.2 EC-G MEMBER AND CONNECTION ROTATION

The inclinometer data for the EC-G test provides a good overview of the behavior of the floor during this test. Inclinometers were placed at the ends and midspans of the two spandrel girders and the beam that attached to the removed column. Figure 3.20 shows the inclinometer and strain gauge placement for this test. Figure 3.21 shows the rotation data for the three members as well as the relative rotation at each connection. Figure 3.21a provides the removed

column displacement throughout the test for reference. The removed column end of the beam (Figure 3.21b) rotated more than the midspan and far end, implying that the composite beam did provide some moment resistance and carried a portion of the load as a cantilever.

The girders rotated more rigidly (Figure 3.21c and Figure 3.21d), with the removed column ends rotating slightly more. The flexural-member-to-column connections at the far ends from the removed column (Figure 3.21e) exhibited similar rotations. At the removed column (Figure 3.21f), the beam connection rotated similarly to the connection at the opposite end of the beam. The east girder connection began with greater rotation, but the west girder caught up and greatly exceeded the east girder connection rotation as the floor failed. In the photo of the final equilibrium (Figure 3.22a) the east girder connection has slightly more rotation, but it can be seen in the post-failure photo (Figure 3.22b) that it was the west girder connection that was weaker and was the first to fail from bolt shear.

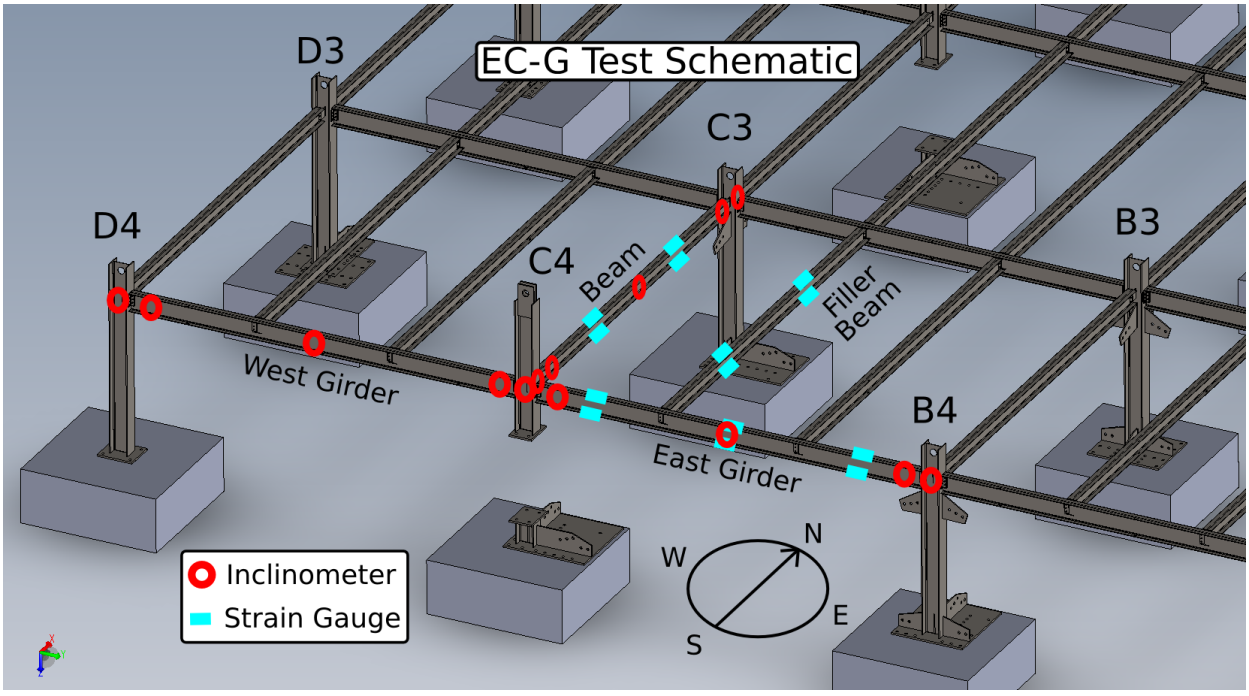

Figure 3.20 EC-G Test Inclinometer and Strain Gauge Placement

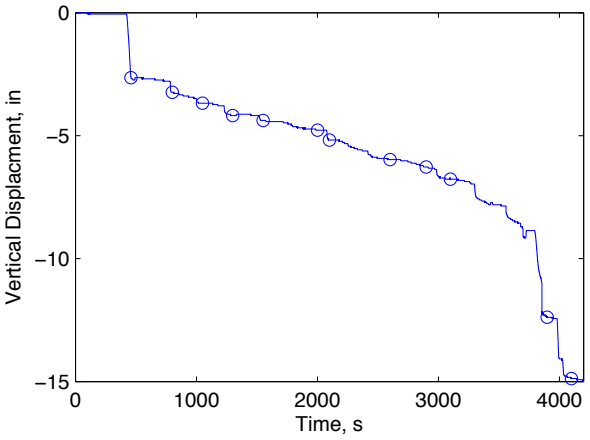

(a) Removed Column Displacement

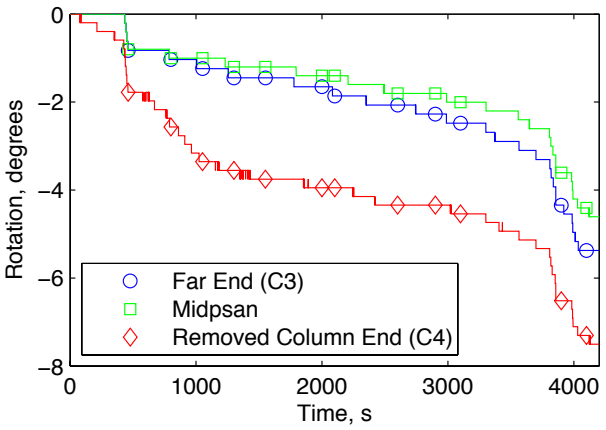

(b) Beam Rotation

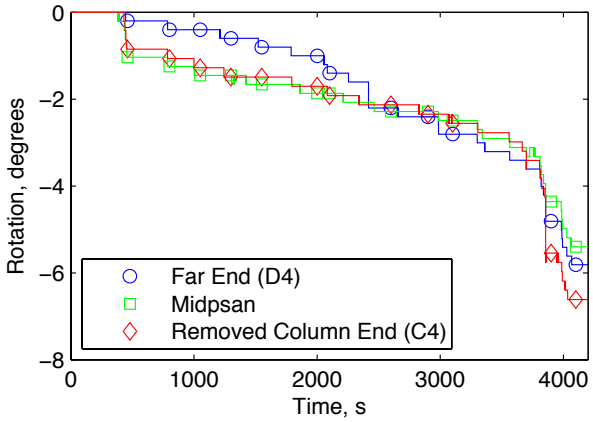

(c) West Girder Rotation

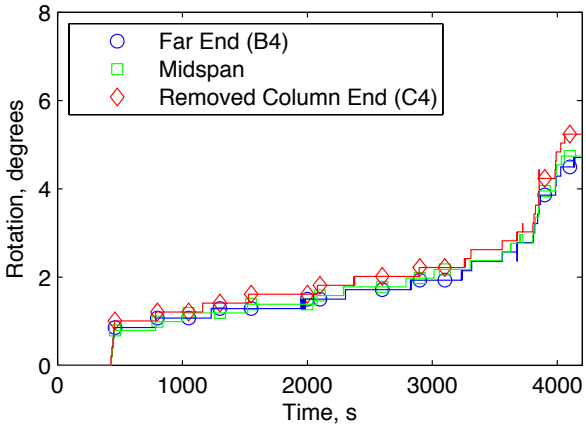

(d) East Girder Rotation

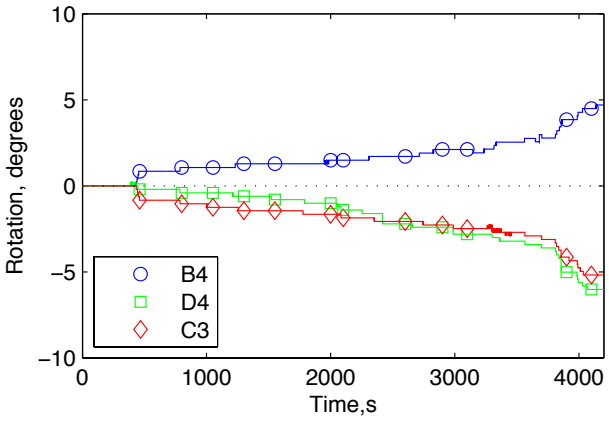

(e) Connection Rotations at Far Columns

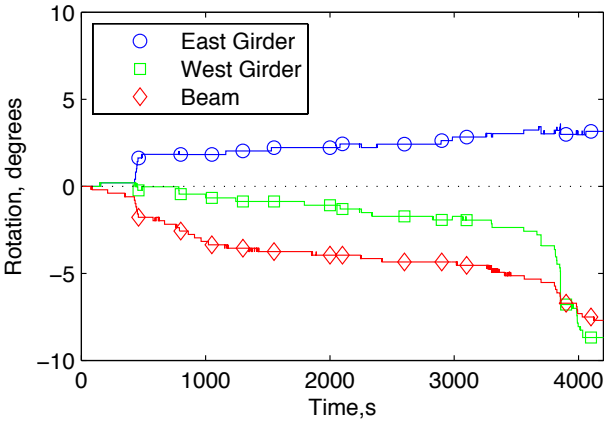

(f) Connection Rotations at C4

Figure 3.21 EC-G Test Removed Column Displacement and Member and Connection Rotations

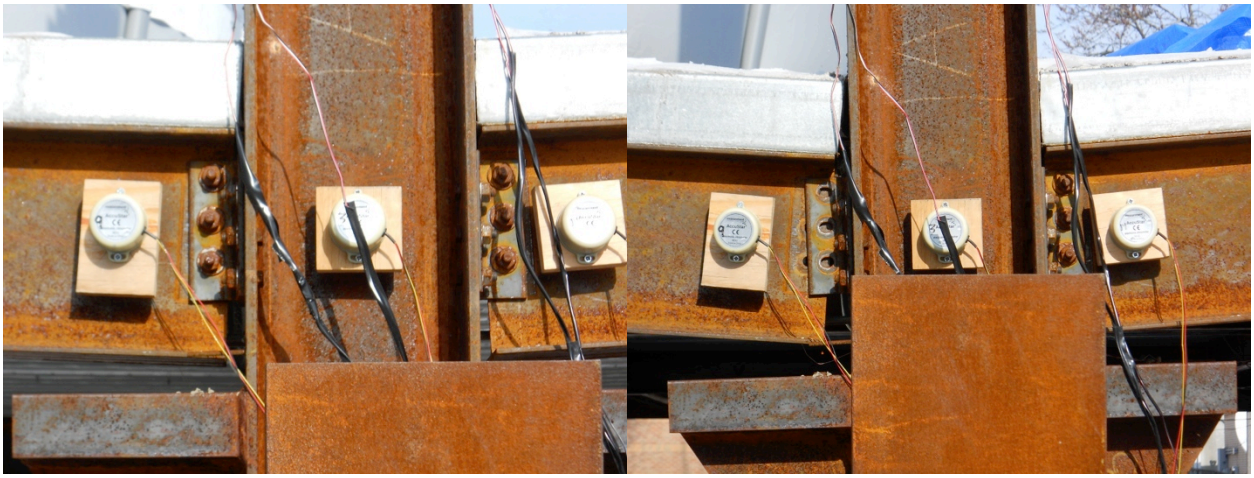

(a) Final Equilibrium (6.3 in. Disp., 84 psf) **(b) Post-failure (15 in. Disp, 89 psf)**

Figure 3.22 EC-G Test Removed Column Connection Deformations

3.3.3.3 EC-G CONNECTION EXTENSIONS

The connection extensions for the EC-G test show how much more even the connection deformations were here than in the EC-B test. Noting that the final equilibrium happened just before the 3000 s mark of the test, Figure 3.23 shows that for both the removed column ends (a) and far ends (b) of the girders, the connection extensions were similar. It is not until the post-failure portion of the test that the west girder connection extension increases greatly.

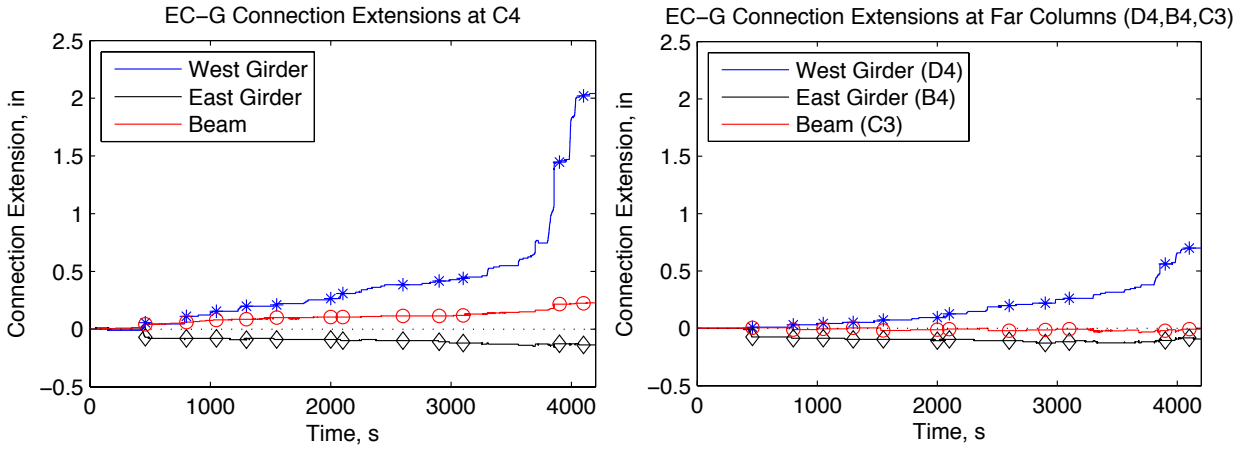

(a) Connections at Removed Column (C4) **(b) Connections at Adjacent Columns**

Figure 3.23 EC-G Test Connection Extensions

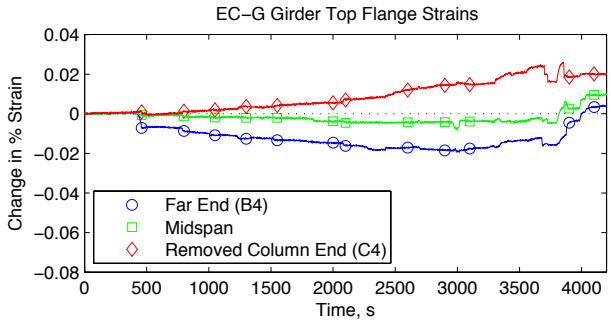

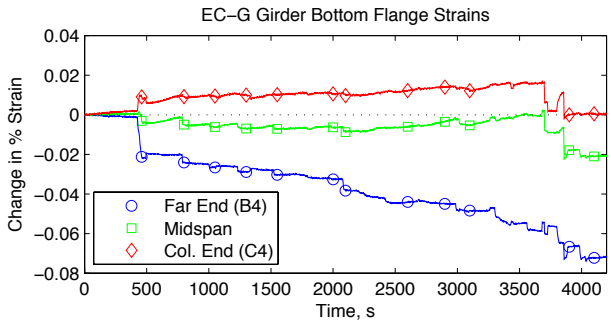

(a) Girder Strains

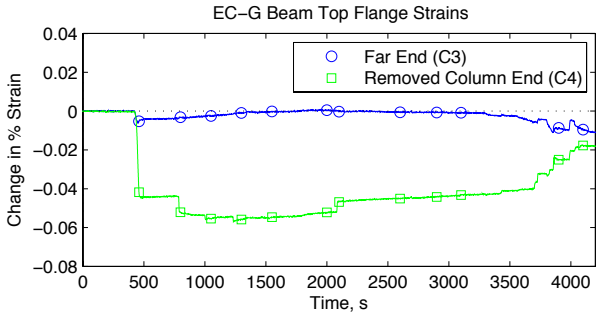

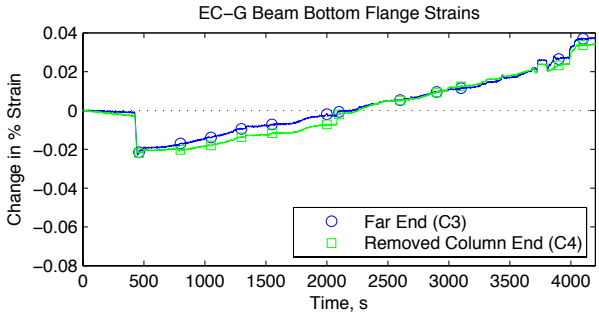

(b) Beam Strains

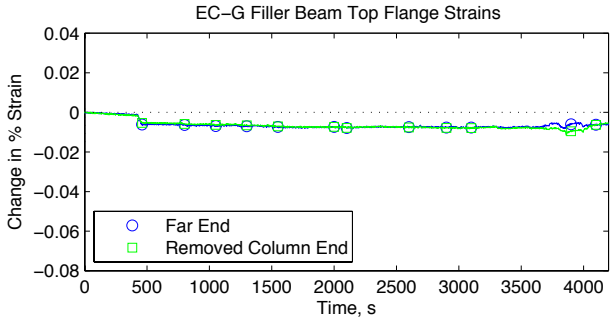

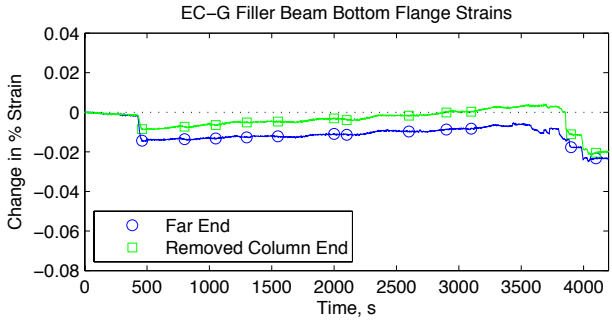

(c) Filler Beam Strains

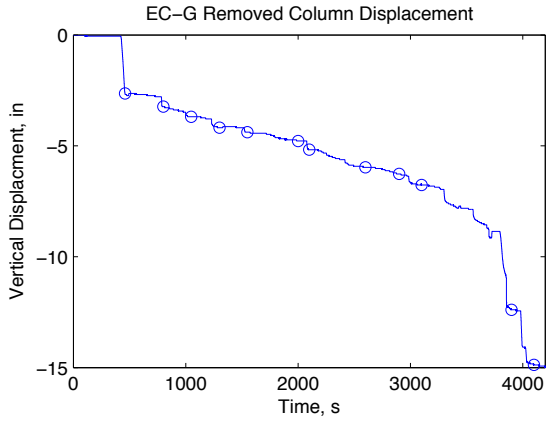

(d) Removed Column for Reference

Figure 3.24 EC-G Test Beam and Girder Strains

3.3.3.4 EC-G MEMBER STRAINS

The strain data recorded from the beams and girders in the EC-G test show how the floor remained composite up to failure. The strain diagrams in Figure 3.24 show change in percent strain with the beginning of the test being the datum. Figure 3.24d shows the removed column displacement for reference; note that floor failure occurs around 3000 s. Figure 3.20 shows the strain gauge arrangement for this test.

The girder strains (Figure 3.24a) changed steadily throughout the test after the column was removed, with no sudden jumps like in the EC-B test. As the load increased through the test, both flanges of the composite girder increased in compression at the far end and midspan. The removed column end increased in tension, suggesting that the tensile tie forces in the spandrel outweighed the compression from cantilever bending. Because the floor remained composite, the magnitude of strain change in the girder in the EC-G test was much smaller than in the non-composite domain of the EC-B test.

The beam and filler beam (Figure 3.24b and Figure 3.24c) strains were generally compressive due to slight cantilevering. The bottom flange of the beam jumped into compression when the column was removed and the floor was lowered to its first equilibrium. After that, the strain changed steadily to tension at both ends.

3.4 INTERIOR COLUMN REMOVAL TEST

3.4.1 SUMMARY

The interior column removal test (IC) was performed on March 20, 2014, after a long, harsh winter delayed the testing schedule by several months. The test began at 10:30 AM CDT and lasted 1.5 hours. The long delay through the winter led to degraded instrument quality for the strain gauges and a few inclinometers. Temperatures dropped to almost -20^{o} F at times in January, which could have caused strain gauge adhesive to crack. Though many strain gauges broke in the winter, the IC test was the most instrumented of all the tests and enough good data was collected to understand the behavior and response of the steel members during the test.

The procedure for the IC test differed from the previous tests. No crane was used for the final test because the available crane could not support the floor load with the longer reach required for an interior column. To remove the column, the floor was jacked up from beneath just enough to slide out the removable column section. The jack was then slowly released until the floor was at its first equilibrium point. The floor had no water load at the time of column removal. Figure 3.25 shows the first equilibrium of the IC test with the column removed.

Figure 3.25 IC Test at First Equilibrium (1.5 in. Displacement, 27 psf)

Without a crane, the floor could not be held static during water loading; the floor deformed as each water load increment was pumped into the pools and the equilibrium deformation reading was taken after each load increment was completed and the floor stopped

deforming. Figure 3.26 shows the displacement at the removed column location during the test. Displacement increased during the loading increments, but plateaus can be seen at each equilibrium when the pumps were off. As predicted, not using a crane led to the loaded bays collapsing (Figure 3.27) since there was nothing to support the floor after its capacity had been exceeded.

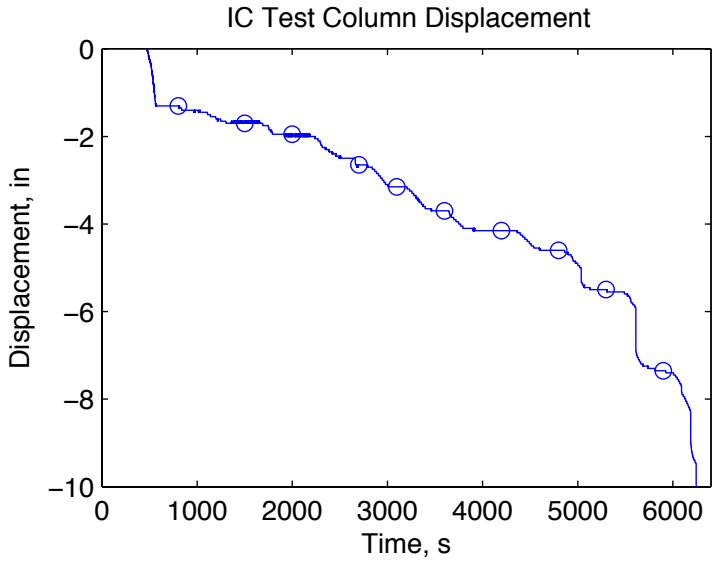

Figure 3.26 IC Test Removed Column Displacement

Figure 3.27 IC Test Collapse

The IC test was expected to have the greatest capacity of all the tests since both the girders and beams provided tie forces to support the floor. Figure 3.28 shows, however, that the maximum sustained load for the IC test was only 67 psf, much less than the nearly 85 psf sustained in the edge column tests. The IC floor collapsed within a minute of the 72 psf load increment being completed. In addition to the reduced capacity, the stiffness in the first deformation domain of the IC test, indicated by the slope of the curve in Figure 3.28, was slightly less than that of the edge column tests. It was determined that the lower strength and stiffness of the IC test was caused by damage in the concrete floor slab as a result of the previous edge column tests. A more detailed explanation is presented in section 4.1.4 .

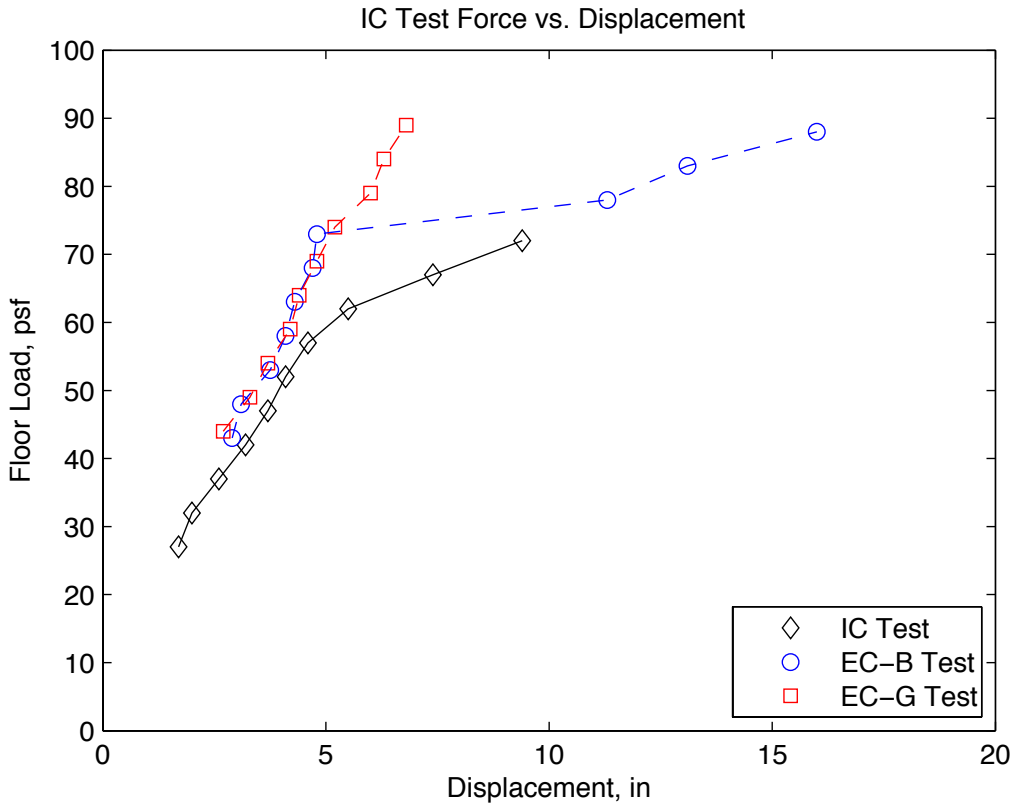

Figure 3.28 IC Test Floor Load vs. Removed Column Displacement (Edge Column Tests Shown for Reference)

3.4.2 IC COLUMN LOADS

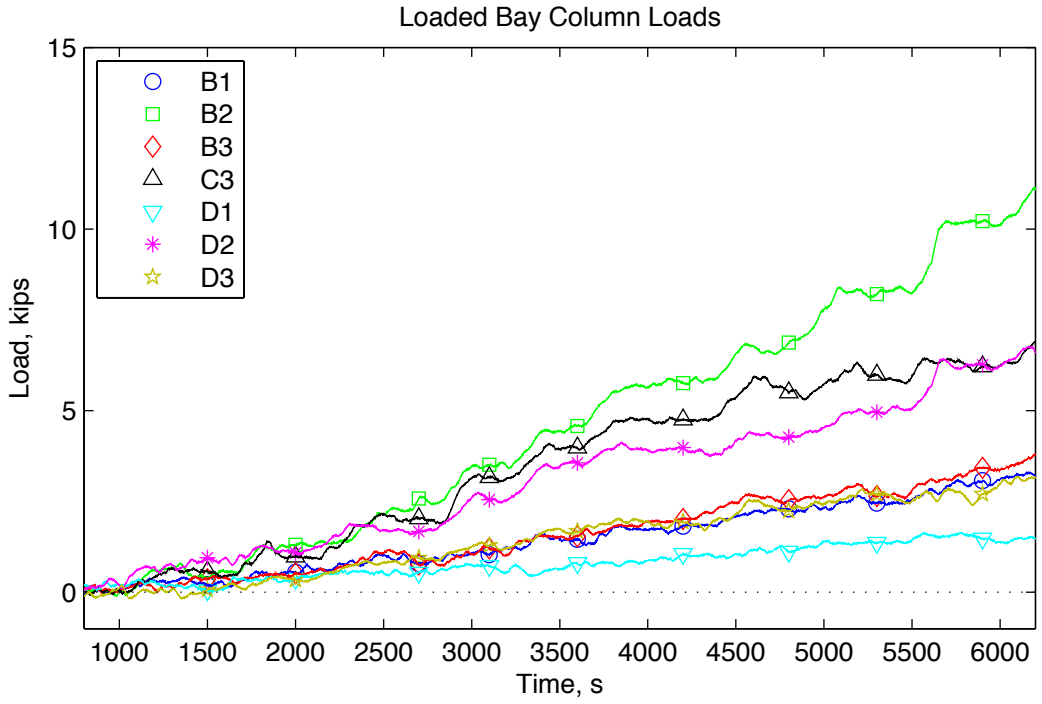

(a) Increase in Individual Column Loads After First Equilibrium

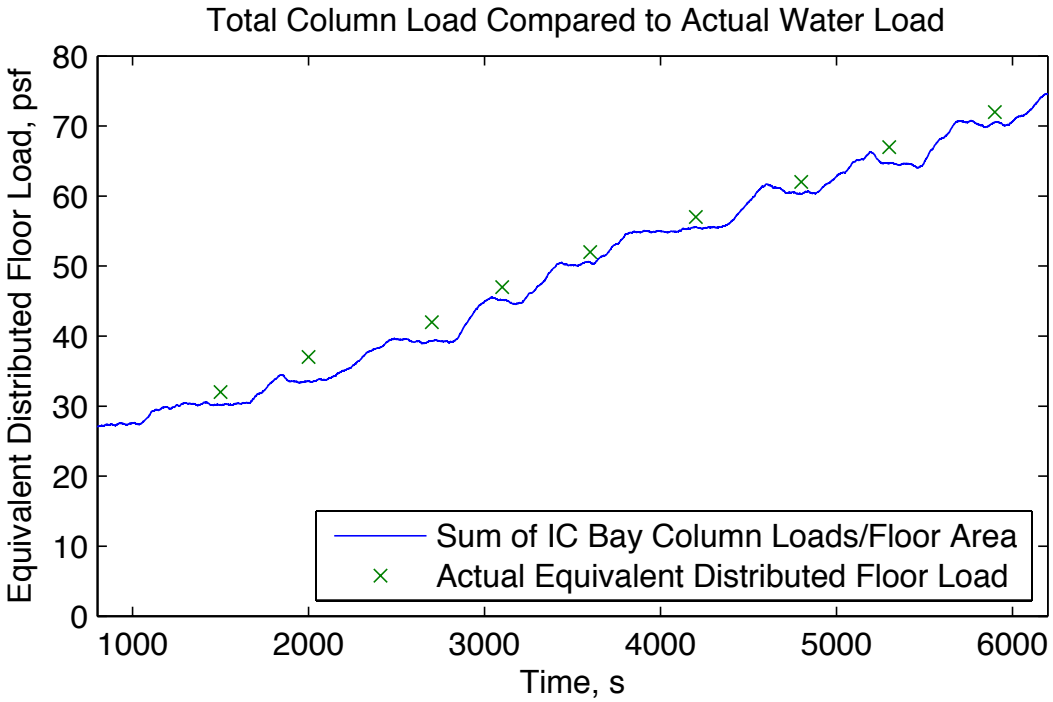

(b) Comparison of Total Measured Column Load and Actual Water Load

Figure 3.29 IC Test Loaded Bay Column Loads

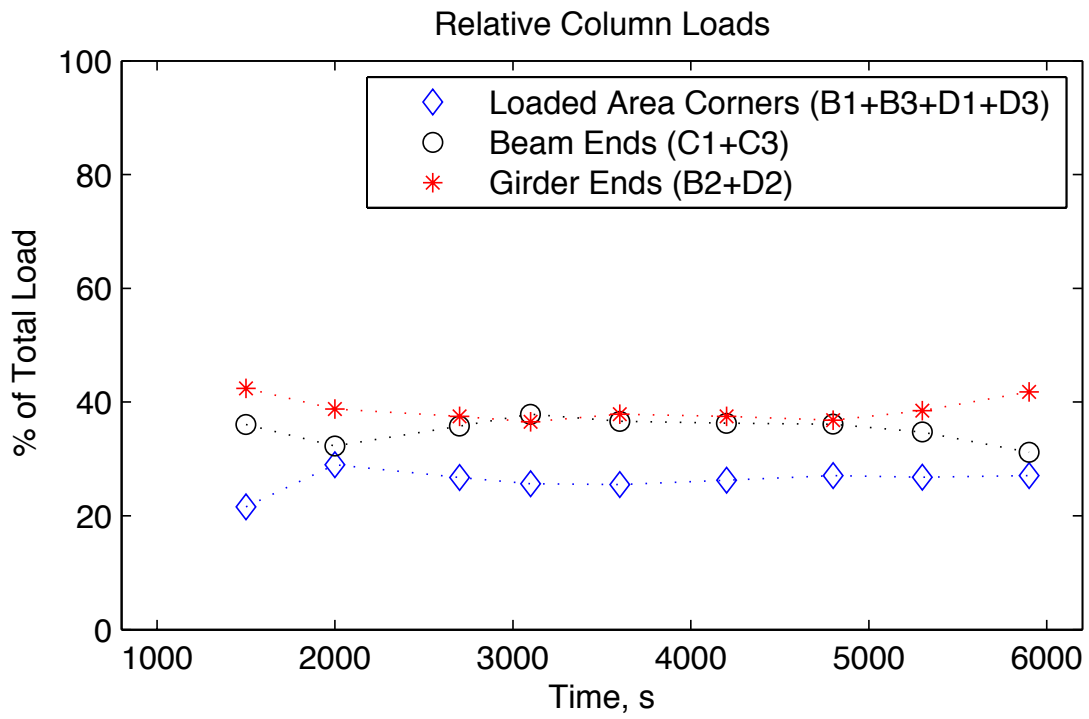

Figure 3.30 IC Test Relative Distribution of Load to Different Column Locations

The column loads measured from the strain gauge bridges (SGBs) were used again in the IC test to find how the floor load redistributed after column loss. The columns supporting the loaded bays in this test were B1, B2, B3, C1, C3, D1, D2 and D3 with C2 being removed. The only nonfunctional SGB for these columns was C1. The assumption made using symmetry was that the load in C1 would be similar to C3, so the C3 load is used for C1 as well. Figure 3.29a shows the individual column loads including the small vertical load component in the diagonal braces. The beam and girder end columns, B2, D2, and C3 (and C1) gain much more load than the corners. To verify the accuracy of this column load data, Figure 3.29b shows that the total measured column load closely matches the actual added water load throughout the test.

Assuming even load distribution in the floor bays, the expected load distribution before column removal would be an equal 25% for the sum of the corner columns (B1+B3+D1+D3), the sum of the girder end columns (B2+D2), the sum of the beam end columns (C1+C3), and the center column (C2). Figure 3.30 shows the load redistribution after the column is removed. The corner columns did not take on more load, keeping about 25% of the total load. The beam and girder ends took the entire load dropped by the removed column. For most of the test, the distribution between the girder and beam columns was even, just shy of 40% of the total load each. Towards the end of the test, when a beam connection was the first to fail, the distribution

shifted so that the beam end columns dropped to around 30% of the load while the girder end columns jumped above 40%. Simulations of load redistribution after interior column loss by Hoffman and Fahnestock (2011) generally agreed. They found that the beam and girder end columns supported 38-44% of the total load per column pair while the load carried by the corner columns did not rise above 30%.

3.4.3 IC MEMBER AND CONNECTION ROTATIONS

In the IC test, the inclinometers were only placed at the ends of the members because a fourth member was instrumented for this test, compared to only three in the edge column tests. Figure 3.31 shows the placement of the inclinometers on the beams, girders, and columns.

The floor displaced around 7.5 in. at the removed column location before it collapsed. (Figure 3.26) A 7.5 in. displacement along the length of a 15 ft. member comes to 2.4º of rigid rotation. Though only the south beam had both inclinometers working, Figure 3.32a-Figure 3.32d show nominally the same amount of rotation in each member. There was equal rotation at both ends of the south beam, implying rigid rotation, and the rotation recorded by the inclinometers at the end of the test was indeed very close to 2.4º. This rigid body rotation was assumed to be typical for the other members as well.

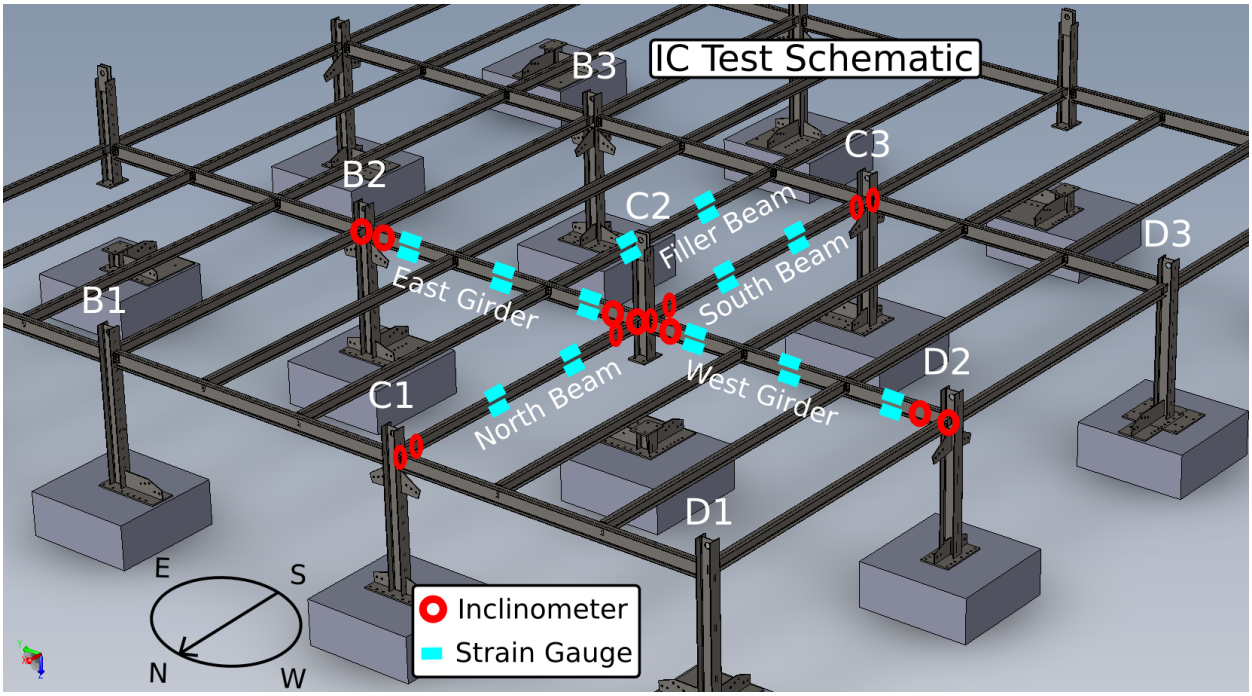

Figure 3.31 IC Test Inclinometer and Strain Gauge Placement

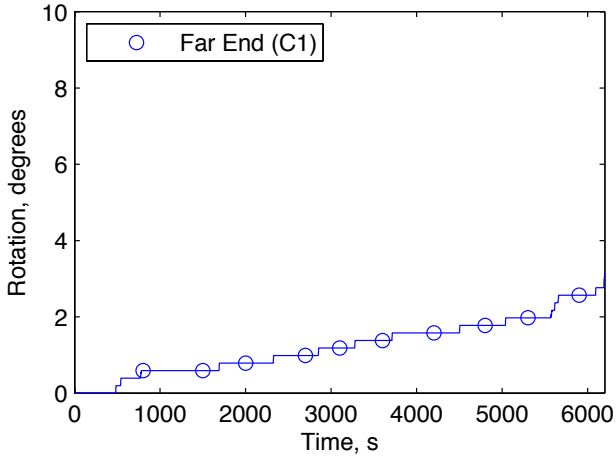

(a) North Beam Rotation

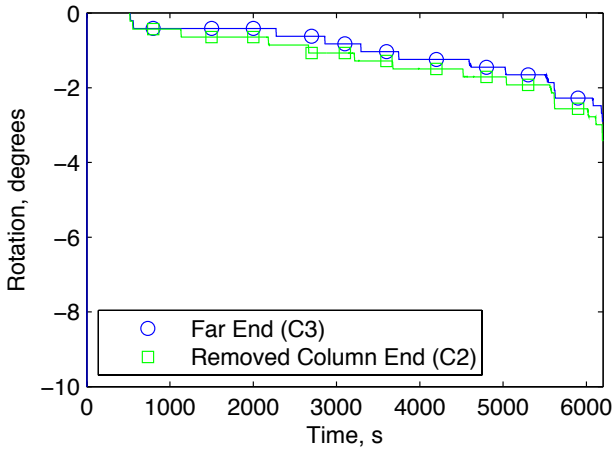

(b) South Beam Rotation

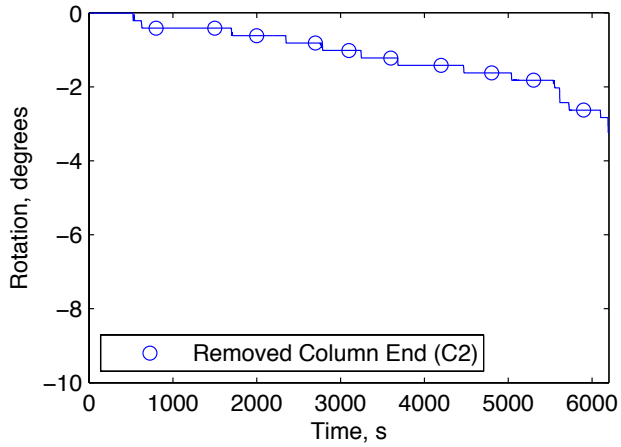

(c) East Girder Rotation

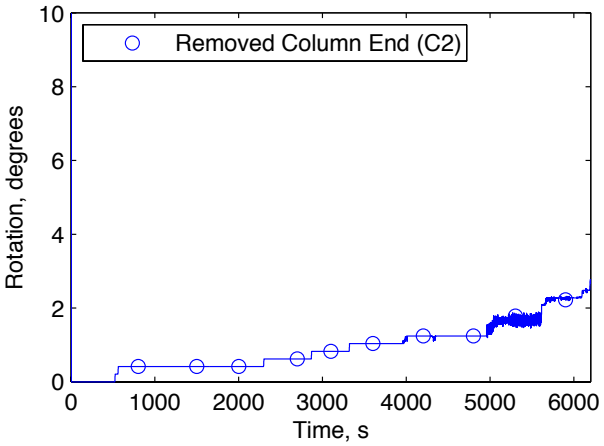

(d) West Girder Rotation

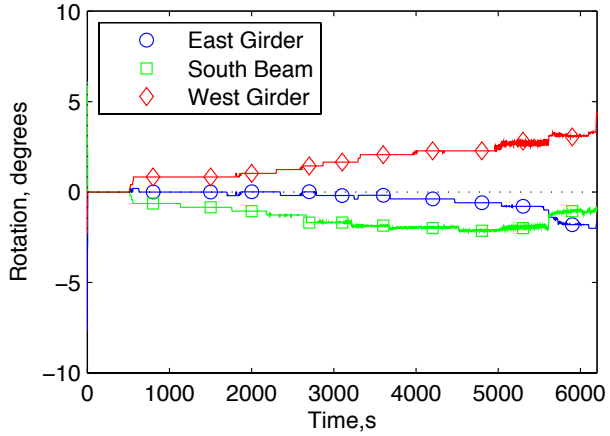

(e) Connection Rotations at C2

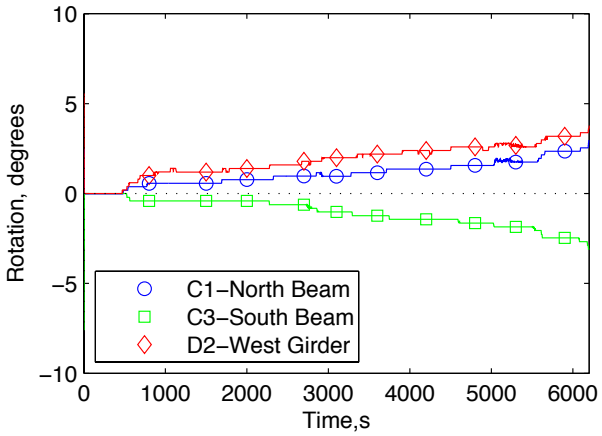

(f) Connection Rotations at Far Columns

Figure 3.32 IC Test Member and Connection Rotations

Because the removed column was connected to members on four sides, the column did not rotate as much as in previous tests. Some connections deformed more than others however. At the removed column connections (Figure 3.32e), the west girder connection deformed much more than the east girder. The south beam connection was the site of the first connection failure. Its rotation increased through the test. The reduction of rotation shown in the figure at the end of the test is not logical, was not visibly observed, and is likely due to one of the inclinometers slipping on its mounting that attached it to the specimen. The north beam connection rotation is not shown because of broken instrumentation. Visual observation during the test showed that the north beam connection rotated significantly less than the south beam connection.

The connection rotations at the far ends of the members from the removed column were much more even. As shown in Figure 3.32f, the two beams rotated essentially the same. Though the east girder had poor quality data recorded, it could be seen that it had the same connection rotation as the west girder because both of the girders rotated so that the bottom flanges were bearing on the columns. (Figure 3.33)

Figure 3.33 IC Test West Girder Bottom Flange Bearing on Column D2

3.4.4 IC CONNECTION EXTENSIONS

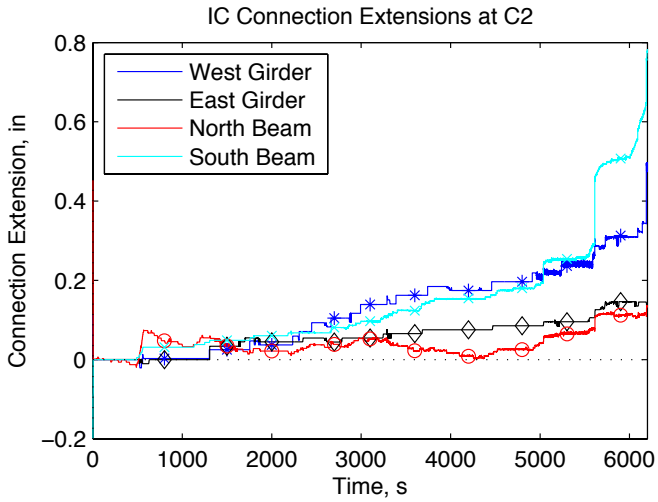

Figure 3.34 IC Test Connection Extensions at Removed Column (C2)

The connection extensions in the IC test were much smaller than in the edge column tests, mostly due to the overall floor displacement being smaller. Figure 3.34 shows the connection extensions at the removed column. The east girder and north beam had small displacements, less than 0.2 in. The south beam and west girder connections had larger extensions. These are the two connections that failed and led to floor collapse. The jump in the south beam connection extension at approximately 5600 seconds marks the failure of the bolts in that connection. The extension increases to 0.8 in. as the floor nears collapse. The west girder connection extension rises to 0.4 in and fails at 6200 seconds, the same time as the floor collapse. The connection extensions at the far columns were very small, and in some cases slightly negative. The negative values are not logical, and are likely due to the assumed center of rotation location used to estimate the extensions.

3.4.5 IC MEMBER STRAINS

Although many strain gauges were damaged, enough good data was still collected because the IC test was more heavily instrumented than any of the prior tests. Complete data was collected from the east girder and partial data was collected from the other three flexural members. The strain diagrams in Figure 3.35 show change in percent strain with the beginning of the test being the datum. Figure 3.31 shows the locations of the strain gauges.

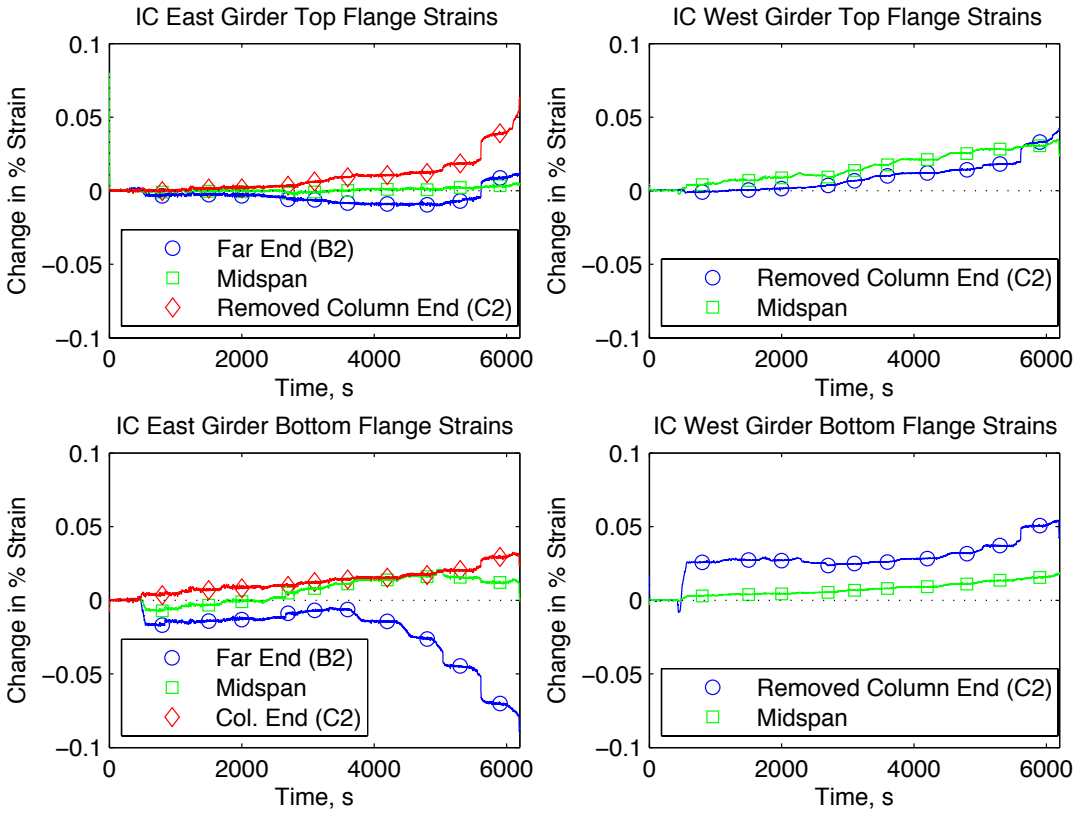

(a) East Girder Strains **(b) West Girder Strains**

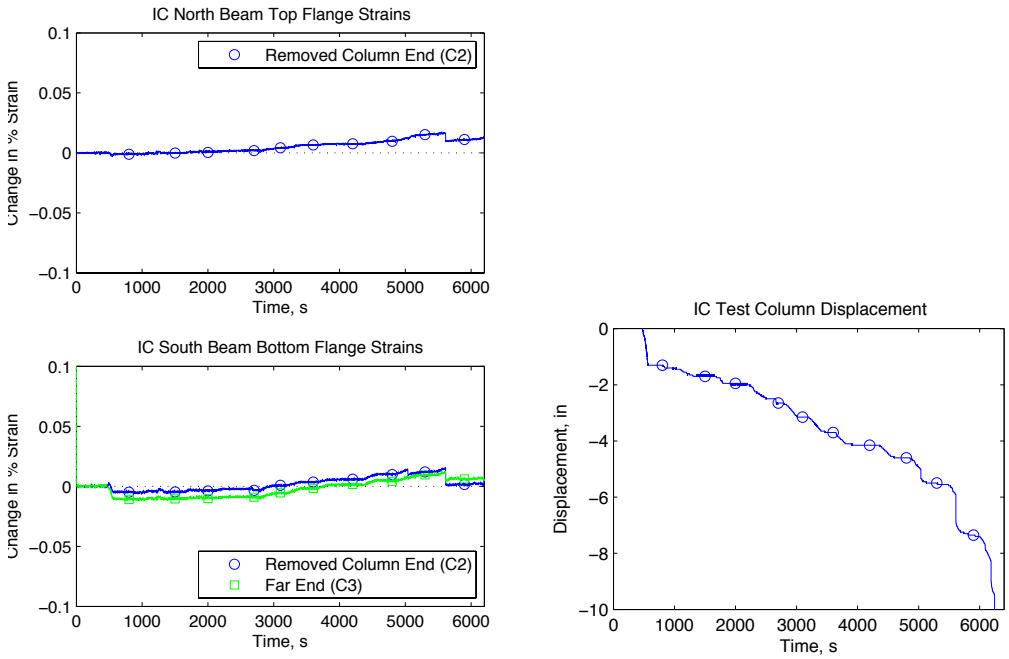

(c) North and South Beam Strains **(d) Removed Column for Reference**

Figure 3.35 IC Test Beam and Girder Strains

Nearly every strain gauge showed tension throughout the test. The east girder (Figure 3.35a) had both flanges go into tension at the midspan and removed column end. The compression in the bottom flange at the far end of the girder developed later in the test once the bottom flange started bearing on the column. The far end gauges of the west girder (Figure 3.35b) did not collect data, but the others show tension similar to the east girder. The two beams only had three working strain gauges between them (Figure 3.35c), but putting the two together assuming similar behavior in both beams provides some insight to their behavior. The top flange at the removed column was always in tension. The bottom flange at both ends started in compression and then transitioned back to tension at the end of the test. Figure 3.35d shows the floor displacement at the removed column location for reference.

CHAPTER 4 - DISCUSSION

4.1 TEST FAILURE MECHANISMS

This section uses the evidence presented in the Experimental Results chapter to form a comprehensive description of the floor behavior during loading and failure of each test. Additional figures, along with the graphs and photos previously shown, are used to create a clearer picture of the series of events during loading that led to floor system failure.

4.1.1 CC TEST FAILURE

With the corner column removed, the corner bay acted as a cantilever with all load resistance coming from bending in the floor, mostly in the composite slab. There was no tie force for corner column removal because the beam and girder lines terminated at the corner. As shown in Figure 4.1, cracking occurred in the floor slab at a 45º angle to the edge of the bay. Although direct visual observation of the slab during the test was not possible, sounds indicative of concrete cracking were heard as the load carrying capacity was lost. As the crane lowered the floor after failure, there was bolt shear at the beam-to-column connection at A3 and prying action in the double-angle at the girder-to-column connection at B4.

Figure 4.1 CC Test Floor Cracking Pattern

The floor failed after the first load increase. The concrete cracked, losing its tensile strength. The filler beams and girder, with single-angle or double-angle connections that provided some rotational resistance, continued resisting load as non-composite steel cantilevers

even after the concrete slab could not provide any more load resistance, but this was not enough to support the loaded floor bay.

4.1.2 EC-B TEST FAILURE

The EC-B test sustained appreciable deformation prior to ultimate failure. Figure 4.2 shows that two distinct domains of behavior were observed during this test. The floor began stiff, but transitioned to ductile deformation when the concrete floor slab cracked. The cracking pattern in the slab (Figure 4.3) was again at 45º angles to the bay edges. Cracks also formed along the perimeter of the loaded section where the loaded bays abutted the intact, unloaded bays.

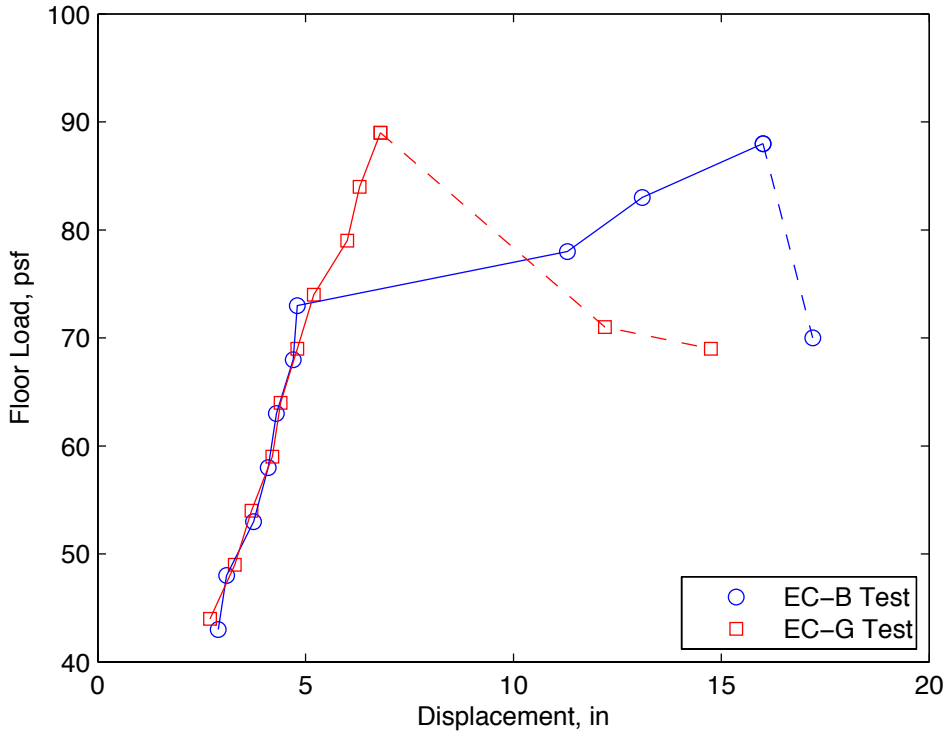

Figure 4.2 Edge Column Tests Floor Load vs. Removed Column Displacement

Figure 4.3 EC-B Test Floor Cracking Pattern

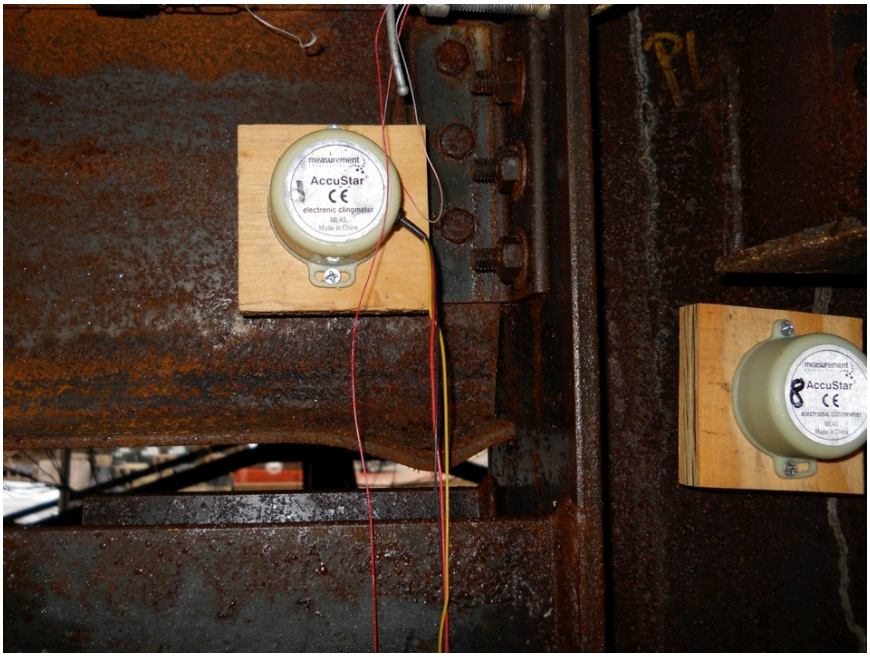

Figure 4.4 EC-B Test Evidence of Girder Flange Bearing on Column

The floor lost composite strength when the concrete cracked. The jump in strain in the girder is a clear indicator of the loss of composite action. The steel members were the only contributors to floor strength in the ductile domain of the EC-B test. The floor displacement increased as the steel connections experienced large rotations and extensions. The bottom flange of the girder began bearing on the flange of column B2 when the girder rotation became great enough. Though the investigators could not closely observe or photograph the interior girder

connection, Figure 4.4 shows the local flange buckling in the girder that occurred while the flange was bearing on the column. The compression of the bearing and the tension in the double angle connection above created a force couple at the girder-to-column connection that enabled further cantilever strength in the girder.

Though it was predicted that the spandrel beams and parallel filler beams would provide tie forces to help support the floor, the results suggest that the cantilevered girder was more important for load resistance. The column that supported the girder, B2, supported a full 50% of the total floor load. This means that nearly all the load initially supported by the edge column before removal transferred through the girder to B2 upon column removal.

The steel connections deformed and failed as the load increased. The most rotated connection (10º at failure) was the north-beam-to-removed-column connection, a shear tab connection with three bolts. The two bottom bolts failed at 73 psf of floor load and the last bolt failed at 78 psf. Any tie forces in the spandrel beam were eliminated when the last bolt failed, but the floor still managed to hold another load increment of 83 psf due to the cantilever strength of the girder.

The floor failed at 88 psf. In each previous load increment the crane load would decrease to zero as the crane lowered the floor to the next equilibrium point. When the crane could not reach zero load, it was clear that the load had exceeded the floor's capacity. Since the girder was apparently resisting practically the entire load at this point, it was failure of the girder that finally led to failure of the whole floor. The local flange buckling pictured in Figure 4.4 was likely the limit state that caused the girder to lose its cantilever capacity.

The crane continued to slowly lower the floor after the floor's capacity was reached so that continued deformation and damage could be observed. The next failure was the bolts of the single-angle filler-beam-to-girder connection in the northern bay just inside of the previous spandrel beam connection failure. With both of those beam connections broken, there was nothing to support the north bay and the floor cracked through its depth along the entire girder line and dropped around 2 inches. (Figure 4.5) If the crane had not supported the removed column, the floor collapse would likely have commenced with the failures that were observed. Instead, the floor was raised back to its initial position so that the subsequent tests could be performed on the specimen.

Figure 4.5 EC-B Test Post-failure Deck Crack on Girder Line

4.1.3 EC-G TEST FAILURE

While the EC-B test had a clear progression to failure, the EC-G test failed faster with a less clear progression. Figure 4.2 shows how the EC-G test had only one domain of deformation, keeping its stiffness to the very end. The steel connections and concrete floor slab failed simultaneously.

Early in the test, the beam and filler beams, connecting the spandrel girders to the interior of the floor, supported some of the load with cantilever action tying into the adjacent floor bays. Through the test, that cantilevering was eliminated and replaced by tension in the beams supporting the floor.

The load resistance in the beams paled in comparison to that of the spandrel girders. The girders supported the floor both as cantilevers and as ties. The girder strain in both flanges increased in compression going back towards the far ends of the girders. This represents the increased moment of a cantilever closer to its anchor. The strains at the removed column end of

the girders were tensile. Here the moment from a cantilever is minimal, and the strains represent the tensile tie forces in the spandrel girder spanning across the removed column location. As the floor displacement increased, the bottom flanges of the girders began to bear on column B4 and D4. (Figure 4.6)

Figure 4.6 EC-G Test West Girder Bottom Flange Bearing on Column D4

The floor failed when the west girder connection to the removed column failed simultaneously with the cracking of the concrete floor slab. At the final equilibrium (Figure 4.7a), the double angle connections at the removed column were prying and rotating. The rotation of the double angles was likely caused by both hole elongation in the girder webs and bolt deformation. The west girder connection experienced more deformation than the east.

Next, the load was increased to 89 psf while the crane held the floor. Cracking was heard when the crane began to lower the floor, indicating the failure of the floor slab. Also at this time, the bottom two bolts of the west girder connection sheared (Figure 4.7b). It is unclear whether the bolt failure preceded the concrete cracking or vice versa. Either way, the failure of one component, shifted the load to the other, causing the second component, and the whole floor system, to fail as well.

(a) Final Equilibrium (6.3 in. Displacement, 84 psf)

(b) Floor Failure (6.8 in. Displacement, 89 psf)

Figure 4.7 EC-G Test Failure

Figure 4.8 EC-G Floor Cracking Pattern

Figure 4.8 shows the very subtle cracking pattern of the floor slab in the EC-G test. The cracks were hard to see because the specimen was raised back to its initial position before people could safely gain access to the floor and make observations. However, moisture in the cracks made them more visible. The cracks were easy to see for the EC-B test (Figure 4.3), but much more difficult for the EC-G, even with these two photos taken on the same day. Looking closely, the investigators could see that the EC-G cracking pattern was similar to the EC-B, but the lack of moisture in the cracks suggests that the EC-G cracks were smaller. This is logical since the EC-G slab cracked at final failure while the EC-B slab cracked early and had time for the cracks to grow as the floor displaced further. The much clearer cracks along the girder line in Figure 4.8 shows where the loaded bay slab separated from the rest of the floor system. These cracks proved crucial to the performance of the floor in the IC test.

4.1.4 IC TEST FAILURE

With the collapse at the unexpectedly low load of 72 psf, it was clear that the test specimen represented an atypical scenario during the interior column removal test. With both a beam line and a girder line providing tie forces as well as four bays to form a diaphragm, the interior column test was expected to hold the most load. Instead, the floor only sustained 67 psf, significantly less than the 83 and 84 psf sustained in the edge column tests. The test photos, observations, and numerical data provide valuable insight into why the IC test failed prematurely.

The key to the low capacity of the IC test was the damage to the concrete floor slab from the previous tests. Estellés (2014) found in her NDT analysis of the CC test (described in section 2.4.3) that the bays adjacent to the corner bay had sustained damage during the CC test. It can be assumed that further damage to the floor occurred during the two edge column tests. In fact, since the loads applied were greater and the number of loaded bays increased, the amount of debonding damage to adjacent bays was likely even greater than Estellés measured after the first test.

The IC test bays were bounded on two sides by bays already loaded to failure during the edge column tests. Cracks formed in the floor slab along the beam and girder lines during those tests, as seen in the lower portion of Figure 4.9. Those pre-existing cracks virtually eliminated any restraint and tie back forces into the adjacent bays from the loaded bays of the IC test. In addition, it is likely that the edge column tests caused some debonding and loss of composite action in the IC test bays.

The experimental results presented in section 3.4 support the hypothesis that much of the composite strength of the IC test bays was lost at the perimeter before the test began. The rotation and strain results of the edge column tests indicated composite cantilever strength in the girders and some beams with the steel members in compression and the floor slab in tension. Development of this cantilever-type action requires negative moment at the perimeters of the tested bays. Evidence of cantilever action was missing from the IC test results. The rotation results showed rigid rotation of the members, meaning no bending and no cantilever strength. The strain diagrams show compression in the steel members only briefly in two places. The bottom flange of the south beam shows a small amount of compression indicating that some cantilever action could have existed, though only briefly. The only other compression is at the

bottom flange of the far end of the west girder. This compression occurred at the end of the test when the girder bottom flange started bearing on the column. This force couple could have provided additional load capacity had the connections at the removed column not failed first. The beneficial effect of bottom flange bearing has been observed in prior simulations of composite floor system behavior under column removal scenarios (Hoffman and Fahnestock, 2011). Besides those two instances of compression, the rest of the steel beams and girders were in tension through their full depth, indicating that it was the tensile tie forces through the beam line and girder line that provided the vast majority of strength for the floor system during the IC test. The cracks that existed on the perimeter of the IC test region as a result of the prior edge column tests eliminated continuity across these boundaries and prevented appreciable negative moment from developing and providing load-carrying capacity.

Figure 4.9 IC Test Floor Collapse Seen from Above

Since it was the tie forces in the beams and girders supporting the floor, the collapse was eventually precipitated by the failure of the ties. Figure 4.10 shows the failed south beam-to-removed column connection at C2. By 62 psf of floor load, all three bolts in that connection had sheared, eliminating the tie force strength of the beam line. At the same time, the west girder-to-

column double-angle connection (also pictured in Figure 4.10) began to experience prying action. The floor held the next load increment of 67 psf, but failed immediately after the pumps finished adding the 72 psf load increment. Video of the collapse shows that the south beam dropped first, immediately followed by the west girder. The collapse was triggered by the failure of the west girder connection, which severed the remaining tie force strength of the girder line.

Figure 4.10 IC Test Failure of South-Beam-to-Removed-Column Connection

4.2 DISCUSSION OF RESULTS

The overall results from the four tests were surprising. The original expectation was that the capacities would in general be much greater, reaching or exceeding the extreme event load combination of 135 psf (1.2D+0.5L). Due to the lack of alternate load paths, the corner column was not expected to hold significant load after column removal, so the 60 psf capacity was not surprising. The stronger edge column removal tests held just about 85 psf, 50 psf short of the extreme event load. The interior column test only held 67 psf, but that lower result was due to prior damage to the floor.

With similar, concurrent, tests at the University of Texas-Austin (Jahromi, et al., 2012) (Hadjioannou, et al., 2013) experiencing much higher capacity, similarities and differences

between the two testing programs are of great interest. The Texas specimens had the same bay size (15 ft x 15 ft) as the Illinois specimens, but other details were different. Instead of one large specimen (3 bays x 3 bays) with multiple testing locations, two smaller specimens (2 bays x 2 bays and 2 bays x 1 bay) were used, one for interior column removal and the other for edge column removal. Instead of having other adjacent, unloaded floor bays to provide restraint, a stiff ring beam was used along the perimeter of the test specimens to provide restraint. This ring beam was designed to replicate the restraint provided by multiple bays of adjacent framing in a prototype building. The floor slab was 4.5 in. of normal-weight concrete (2.5 in. topping on 2 in. deck), compared to 3.125 in. of lightweight concrete (1.625 in. topping on 1.5 in. deck) at Illinois. Texas also placed rebar in the slab along the beam and girder lines while Illinois only used welded wire fabric for reinforcement. The capacities of all of the tests at Texas exceeded 150 psf, as presented at the 2014 Structures Congress, much greater than both the Illinois results and the extreme event load combination (135 psf) used for the tests and analysis at Illinois.

The two main differences between the two test designs were the floor slab detailing and the perimeter restraints. It could be that the perimeter restraints employed at Texas were much stronger than the adjacent floor bays used at Illinois, but the researchers at Texas put a lot of effort into making their restraints behave similarly to adjacent floor bays. The difference in results is more likely derived from the different concrete details.

All four tests at Illinois showed how much the strength of the composite floor slab contributes to the capacity of the system. The steel deck, welded wire fabric, and concrete provided almost all of the strength in the CC test, caused the loss of stiffness in the EC-B test, and marked the overall failure in the EC-G test. The IC test showed that the absence of composite slab strength greatly reduces the overall floor capacity. Having nearly 1.5 in. of additional slab depth, coupled with more robust reinforcement, likely contributed significantly to the big differences between the Illinois and Texas tests. Additionally, Alashker et al. (2010) found through simulations of column loss in composite floor systems that 60% of the floor load was carried as tension in the steel deck when the deck was modeled as continuous. The deck in the Illinois specimen was not continuous and it pulled apart at the seams during the column removal tests. Providing stronger continuity in the steel decking by using stronger puddle welds and stud welds and staggering the placement of the decking panels could have increased the capacity of the floor system.

The floor system at Illinois was designed to be "worst-case," using the minimum design as required by code. Thus the common practice of adding reinforcing bars to the floor, especially on the beam and girder lines as seen in the Texas floor, was omitted. Since this reinforcing would contribute to negative moment and tie force strength at the perimeter of column removal bays, it appears to be an important detail and the lack of rebar in the Illinois floor slab could have resulted in cracking and loss of strength at much lower loads than in the Texas floor.

The failures of the steel connections were essentially the same in each test at Illinois. While there are many ways for a steel connection to fail, all of the failures were due to bolt shear. Hole elongation was observed at many locations, but the bolts always sheared before there was tear-out of connected elements, even with the shear tabs only being 1/8 in. thick in the half-scale specimen. The girder and filler beam connections experienced prying action, but again it was bolt shear that was the ultimate connection failure. Although the A449 bolts used in the testing program had nominally the same composition and mechanical properties as A325 bolts, component connection tests conducted at the University of Washington by Weigand (2014) indicate that the A449 bolts in half-scale connections failed at smaller deformations than corresponding A325 bolts in full-scale connections. It is possible that bolts with greater ductility could have delayed the steel connection failure and increased the capacity of the floor system in each test.

Although when viewed in isolation, the results of the experiments at the University of Illinois suggest that gravity framing systems do not provide sufficient structural integrity to carry the full extreme event design load combination when a column is lost, it is important to remember that these floor systems are designed as pin-ended members with no expectation of collapse prevention if a column is lost. The floor did not hold 135 psf, but it was able to resist a significant amount of load. With further experimentation and modeling, design enhancements can be identified to increase the floor capacity to resist the extreme event load when a column is lost. In addition, shortcomings of the testing program, as discussed below, likely contributed to the somewhat pessimistic view of composite floor system capacity under column removal scenarios.

4.3 SHORTCOMINGS OF THE TESTING PROGRAM

As painstakingly designed as the specimen and test procedure were, shortcomings due to budget, space and time limitations were a reality during the project. Clearly, a full-scale

specimen would have provided the most accurate results since all components would have been sized correctly. Although the scaling process was reasonable, no scaled specimen can provide as accurate results as one that is full-scale. A full-scale specimen was not possible because it would have been prohibitively expensive and there was no space available that could accommodate a 90 ft. square test specimen.

Although the loading scheme was relatively simple, it also had limitations. The water in the loading pools ponded when the floor displaced, which produced uneven and constantly changing loads on the floor bays that are not representative of typical gravity loading that would remain essentially constant. Loading methods that kept the floor load uniform were considered, but ultimately judged to be infeasible.

Other shortcomings arose during the testing process. In the first three tests, the removed column rotated because other floors did not brace it. Providing bracing would have added significant cost to the test specimen. The final shortcoming of the experiments was the floor damage from prior tests decreasing the capacity of subsequent tests, mainly the IC test. Using multiple test specimens would have been ideal, but it was not possible within the constraints of the project budget. Future modeling of the experiments will evaluate the impacts of these limitations.

4.4 FURTHER RESEARCH

The next step for this research is to conduct an extensive suite of companion numerical simulations. These numerical simulations will first study the experiments comprehensively, including atypical loading, boundary conditions and effects of test sequence. Once the numerical model is calibrated to and validated by the experimental results, it can be expanded to test other design configurations and load patterns. Other connection designs, like those tested by Weigand (2014) at the University of Washington, should be added to the floor system model so superior connection designs for collapse prevention can be identified. Modifications to concrete floor slab thickness and reinforcement detailing should be investigated as well. This modeling effort will allow for reconciliation of the seemingly discordant test results that have been obtained in the programs at Illinois and Texas. Ultimately, another set of experiments that build on the test results and numerical simulations at Texas and Illinois could be performed to increase confidence in the understanding of disproportionate collapse prevention in steel gravity framing systems.

CHAPTER 5 - CONCLUSION

Experimental testing at the University of Illinois at Urbana-Champaign concluded the experimental portion of a collaborative study investigating the structural integrity of steel-concrete composite gravity framing systems under column loss scenarios. Specifically, framing systems for typical commercial building designs that do not have existing progressive collapse requirements were studied. Colleagues at Purdue University and the University of Washington conducted component tests on steel-concrete composite slabs and steel gravity beam-to-column connections, respectively. The researchers at Illinois constructed a half-scale floor system and tested the floor capacity under column loss for a corner column, an edge column with spandrel beams, an edge column with spandrel girders, and an interior column. In each test, the adjacent floor bays that were supported by the removed column were loaded incrementally by pumping water into swimming pools erected on each floor bay. The four experimental tests (Table 5.1) all failed much lower than the code defined extreme event load combination (1.2D+0.5L), which was 135 psf for the chosen load magnitudes (D = 92 psf and L = 50 psf). However, the interior column removal test had a lower capacity due to floor damage caused by the previous tests.

Table 5.1 Summary of Experimental Results

Configuration	Max. Sustained Load	Displacement at Max. Load
Corner Column	60 psf	8.25 in.
Edge Column-Spandrel Beams	83 psf	13 in.
Edge Column-Spandrel Girders	84 psf	6.25 in.
Interior Column*	67 psf	5.5 in.
Extreme Event Load: 1.2D+0.5L	135 psf	N/A

*IC test capacity was greatly reduced due to floor damage from prior tests

These results differ greatly from similar tests at the University of Texas-Austin, and further modeling, experiments, and collaboration will be needed to resolve the differences between the two testing programs and gain a more certain understanding of structural integrity of composite floor systems under column loss scenarios. Though typical gravity framing systems are designed to be efficient for standard loading and are not specifically designed to prevent collapse under extreme loading scenarios, there is robustness and reserve capacity in the connections and composite floor system that can contribute to collapse prevention. However, the experimental results presented in this thesis indicate that design enhancements may be necessary to increase the robustness and reserve capacity of floor systems so that they will not collapse under the extreme event load combination.

APPENDIX A – DETAILED ANCILLARY TEST RESULTS

A.1 STEEL COUPON TESTS

Specimen	Thickness *T (in)*		Width *W (in)*		Cross-Section Area *(in^2)*		Yield Strength *kips*	Ultimate Strength *kips*	Yield Stress *ksi*	Ultimate Stress *ksi*
	Avg	*Min*	*Avg*	*Min*	*Avg*	*Min*				
D1	0.030	0.029	0.502	0.502	0.015	0.015	0.67	0.88	46.0	60.4
D2	0.032	0.031	0.500	0.499	0.016	0.015	0.685	0.87	44.3	56.4
D3	0.029	0.028	0.500	0.499	0.014	0.014	0.67	0.87	48.0	62.1
D4	0.030	0.03	0.500	0.499	0.015	0.015	0.68	0.88	45.4	58.7
6x9F1	0.217	0.215	1.006	1.004	0.219	0.216	11.2	16.44	51.9	76.2
6x9F2	0.216	0.215	1.008	1.007	0.218	0.217	11.2	16.55	51.7	76.4
6x9F3	0.210	0.209	0.998	0.997	0.209	0.208	11.1	16.11	53.3	77.3
6x9F4	0.203	0.202	1.001	0.998	0.203	0.202	10.75	15.56	53.3	77.2
6x9W1	0.175	0.173	1.506	1.502	0.263	0.260	13.8	19.98	53.1	76.9
6x9W2	0.173	0.173	1.507	1.505	0.261	0.260	14	20.09	53.8	77.2
6x9W3	0.179	0.177	1.510	1.508	0.270	0.267	13.9	20.14	52.1	75.4
6x9W4	0.179	0.175	1.502	1.497	0.268	0.262	13.9	19.90	53.1	76.0
8x10F1	0.207	0.206	1.006	1.002	0.209	0.206	10.15	13.24	49.2	64.1
8x10F2	0.195	0.195	1.009	1.007	0.197	0.196	9.3	12.51	47.4	63.7
8x10F3	0.200	0.199	1.009	1.006	0.202	0.200	9.65	12.86	48.2	64.2
8x10F4	0.199	0.198	1.000	0.999	0.199	0.198	9.5	12.58	48.0	63.6
8x10W1	0.168	0.166	1.490	1.49	0.250	0.247	12.15	15.68	49.1	63.4
8x10W2	0.161	0.16	1.504	1.502	0.243	0.240	12.5	15.76	52.0	65.6
8x10W3	0.162	0.161	1.501	1.491	0.243	0.240	12.1	15.67	50.4	65.3
8x10W4	0.161	0.16	1.485	1.483	0.239	0.237	12.4	15.70	52.3	66.2
8x24F1	0.395	0.393	1.006	1.002	0.398	0.394	19.3	25.94	49.0	65.9
8x24F2	0.402	0.399	1.003	1.001	0.404	0.399	19	26.14	47.6	65.4
8x24F3	0.412	0.412	1.003	1.003	0.413	0.413	19.3	26.68	46.7	64.6
8x24F4	0.427	0.423	1.004	1.003	0.428	0.424	20	26.82	47.1	63.2
8x24W1	0.246	0.244	1.007	1.005	0.248	0.245	13.3	16.78	54.2	68.4
8x24W2	0.241	0.241	1.006	1.002	0.242	0.241	12.2	16.07	50.5	66.5
8x24W3	0.243	0.242	1.003	1.002	0.243	0.242	12.1	15.97	49.9	65.9
WWF1	0.131	0.127	na	na	0.013	0.013	na	1.32	na	103.9
WWF2	0.124	0.122	na	na	0.012	0.012	na	1.09	na	93.2

A.2 DECK CONCRETE TESTS

	Compression Test				Split Cylinder Test			
Test	**Truck**	**Cylinder**	**Load**	**f'_c (psi)**	**Truck**	**Cylinder**	**Load**	**f_t (psi)**
3 Day Test 6/24/2013	1	1	32055	2551	1	1	19814	394
	1	2	38799	3088	1	2	17046	339
	1	3	42121	3352	1	3	15227	303
	2	1	27626	2198	2	1	15958	317
	2	2	31106	2475	2	2	19399	386
	3	1	39095	3111	3	1	25233	502
	3	2	41350	3291	3	2	16512	328
		mean	36022	2867		**mean**	18456	367
		std. dev.	5674	451		**std. dev.**	3442	68
7 Day Test 6/28/2013	1	1	48073	3826	1	1	21812	434
	1	2	51079	4065	1	2	17758	353
	1	3	36643	2916	1	3	26637	530
	2	1	43248	3442	2	1	17916	356
	2	2	50813	4044	2	2	18984	378
	3	1	50328	4005	3	1	22840	454
	3	2	46788	3723	3	2	21555	429
		mean	46710	3717		**mean**	21072	419
		std. dev.	5231	416		**std. dev.**	3167	63
28 Day Test 7/19/2013	1	1	55832	4443	1	1	29140	580
	1	2	68383	5442	1	2	29980	596
	1	3	64724	5151	1	3	23880	475
	2	1	61323	4880	2	1	28410	565
	2	2	56992	4535	2	2	17920	357
	3	1	63320	5039	3	1	25190	501
	3	2	53512	4258	3	2	22816	454
		mean	60584	4821		**mean**	25334	504
		std. dev.	5346	425		**std. dev.**	4262	85
CC Test 11/15/2013	1	1	41567	3308	1	1	21270	423
	1	2	66880	5322	1	2	23640	470
	1	3	70083	5577	1	3	29300	583
	2	1	70083	5577	2	1	20760	413
	2	2	59187	4710	2	2	22030	438
	3	1	57724	4594	3	1	22050	439
	3	2	57981	4614	3	2	22190	441
		mean	60501	4814		**mean**	23034	458
		std. dev.	9988	795		**std. dev.**	2904	58

(Continued on next page)

	Compression Test				Split Cylinder Test			
Test	**Truck**	**Cylinder**	**Load**	**f'_c (psi)**	**Truck**	**Cylinder**	**Load**	**f_t (psi)**
EC-B Test 12/4/2013	1	1	59581	4741	1	1	28670	570
	1	2	67809	5396	1	2	18250	363
	1	3	27705	2205	1	3	24540	488
	2	1	52839	4205	2	1	18870	375
	2	2	51870	4128	2	2	22020	438
	3	1	54659	4350	3	1	15820	315
	3	2	70716	5627	3	2	22410	446
		mean	55026	4741		**mean**	21511	428
		std. dev.	14093	637		**std. dev.**	4311	86
EC-G Test 12/11/2013	1	1	49774	3961	1	1	26760	532
	1	2	50466	4016	1	2	30780	612
	1	3	65555	5217	1	3	29160	580
	2	1	57902	4608	2	1	23540	468
	2	2	57309	4561	2	2	25100	499
	3	1	81771	6507	3	1	30870	614
	3	2	74652	5941	3	2	23430	466
		mean	62490	4973		**mean**	27091	539
		std. dev.	12133	965		**std. dev.**	3221	64
IC Test 3/20/2014	1	1	46412	3693	1	1	19990	398
	1	2	54323	4323	1	2	21750	433
	1	3	50823	4044	1	3	20150	401
	2	1	54323	4323	2	1	18250	363
	2	2	51949	4134	2	2	22450	447
	3	1	74723	5946	3	1	20390	406
	3	2	59814	4760	3	2	20970	417
		mean	56052	4461		**mean**	21062	419
		std. dev.	9182	731		**std. dev.**	1048	21

A.3 FOOTING CONCRETE TESTS

Cylinder Number	Load (lbs)	f'_c (psi)	
1	42971	3420	
2	65733	5231	
3	44890	3572	
4	58021	4617	
5	76174	6062	
6	44505	3542	
7	38321	3049	Outlier
8	69391	5522	
9	37553	2988	Outlier
10	82107	6534	
mean	60474	4812	
std. dev.	15268	1215	

REFERENCES

Alashker, Y., El-Tawil, S., & Sadek, F. (2010, October). Progressive Collapse Resistance of Steel-Concrete Composite Floors. *Journal of Structural Engineering* , 1187-1196.

American Institute of Steel Construction. (2010, June 22). AISC 360-10: Specification for Structural Steel Buildings.

Astaneh-Asl, A., Jones, B., Zhao, Y., & Hwa, R. (2001). *Progressive Collapse Resistance of Steel Building Floors.* University of California at Berkeley, Department of Civil and Environmental Engineering.

DoD. (2013). Design of Buildings to Resist Progressive Collapse, Unified Facilities Criteria (UFC) 4- 023-03 (2009, with 2013 Update). Department of Defense.

Estellés, A. M. (2014). *Detection of flaws on concrete structures by non-destructive testing : analysis of stress wave methods and Nitto Hammer.* University of Illinois at Urbana-Champaign, Civil and Environmental Engineering.

GSA. (2003). *Progressive Collapse Analysis and Design Guidelines for New federal Office buildings and Major Modernization Projects.* General Services Administration.

Hadjioannou, M., Donahue, S., Williamson, E. B., Engelhardt, M. D., Izzudin, B., Nethercot, D., et al. (2013). Experimental Evaluation of Floor Slab Contribution in Mitigating Progressive Collapse of Steel Structures. *WIT Transactions on The Built Environment* , 615-626.

Hoffman, S. T., & Fahnestock, L. A. (2011). Behavior of Multi-Story Steel Buildings Under Dynamic Column Loss Scenarios. *Steel and Composite Structures , 11* (2), 149-168.

Jahromi, H. Z., Izzuddin, B. A., Nethercot, D. A., Hadjioannou, M., Williamson, E. B., Engelhardt, M., et al. (2012). Robustness Assessment of Building Structures Under Explosion. *Buildings* , 497-518.

Johnson, E. S., Weigand, J., Francisco, T., Fahnestock, L. A., Liu, J., & Berman, J. W. (2014). Large-Scale Testing of a Steel-Concrete Composite Floor System under Under Column Loss Scenarios. *2014 Structures Congress.* Boston: Strucutral Enginering Institute of ASCE.

Levy, M., & Salvadori, M. (1992). *Why Buildings Fall Down.* New York: W. W. Norton & Company.

Main, J. A., & Sadek, F. (2012). *NIST Technical Note 1749: Robustness of Steel Gravity Frame Systems with Single-Plate Shear Connections.* National Institute of Standards and Technology, U.S. Department of Commerce.

Meissner, J. (2012). Personal Communication, Prototype System Designs.

Song, B. I., Sezen, H., & Giriunas, K. A. (2010). Experimental and Analytical Assessment on Progressive Collapse Potential of Two Actual Steel Frame Buildings. *2010 Structures Congress* (pp. 1171-1182). American Society of Civil Engineers.

Weigand, J. M. (2014). *The Integrity of Steel Gravity Framing System Connections Subjected to Column Removal Loading.* P.h.D Dissertation in Civil Engineering, University of Washington, Seattle.

Weigand, J. M., Francisco, T., Johnson, E. S., Fahnestock, L. A., Liu, J., & Berman, J. W. (2013). Large-Scale Experimental Evaluation of Steel Gravity Framing Structural Integrity. *Structures Congress 2013* (pp. 32-42). Pittsburgh: Structural Engineering Institute of ASCE.